Modeling the Distribution of Palmer's Agave (*Agave palmeri*) throughout the Sympatric Summer Ranges of Migratory Nectarivorous Bats (Phyllostomidae: Glossophaginae) using Presence-only Species Distribution Modeling

by

Rachel A. Burke

B.A., Environmental Economics, Saint Lawrence University, 2010

Master's Thesis
Submitted in Partial Fulfillment of the
Requirements for the Degree of
Master of Applied Geography
New Mexico State University
Las Cruces, NM
May, 2017

“Modeling the Distribution of Palmer’s Agave (*Agave palmeri*) throughout the Sympatric Summer Ranges of Migratory Nectarivorous Bats (Phyllostomidae: Glossophaginae) using Presence-only Species Distribution Modeling,” a thesis prepared by Rachel Burke in partial fulfillment of the requirements for the degree Master of Applied Geography, has been approved and accepted by the following:

Loui Reyes

Dean of the Graduate School

Christopher Brown

Chair of the Examining Committee

Date

Committee in charge:

Dr. Christopher Brown, Chair

Dr. Carol Campbell

Dr. Kathryn E. Stoner

ACKNOWLEDGEMENTS

Funding for this project came from T&E Inc., New Mexico Native Plant Society Otero Chapter, New Mexico Association of Conservation Districts, and the Department of Fish, Wildlife and Conservation Ecology at New Mexico State University. This project was also made possible by a career development grant from the American Association of University Women.

I would like to thank my Applied Geography thesis committee for their guidance with this project, Dr. Christopher Brown, Dr. Carol Campbell, and Dr. Kathryn Stoner. I would also like to thank Dr. Brown and Dr. Stoner for allowing me to pursue my research goals as a dual degree student in Applied Geography and Fish, Wildlife and Conservation Ecology. I would also like to thank Dr. Jennifer Frey of my Fish, Wildlife and Conservation Ecology Committee for her support and guidance with modeling methods, and also Dr. Amy Ganguli and Dr. Patrick Alexander for general project guidance. Field work for this project would not have been possible without my field assistant, Chelsey Trejo, who assisted with transects no matter how many lightning bolts or venomous snakes. The hospitality provided by the Butler Family who hosted us at their ranch in the San Rafael Valley was paramount to maintaining morale while conducting field work during monsoon season.

Lastly, I’d like to thank my family for all of their support throughout my graduate program, and my partner Josh for helping me stay relatively sane throughout this process.

VITA

August 2, 1988	Born in Glens Falls, New York
2006	Graduated from Hudson Falls High School
2010	Graduated from Saint Lawrence University Canton, New York B. A. Environmental Studies and Economics
2010 – 2011	Farm Hand, River Road Gardens Tucson, Arizona
2011	Service Project Leader, Canyonlands Field Institute Moab, Utah
2011	Restoration Intern, Plateau Restoration Moab, Utah
2012	Rock Climbing Instructor, Farm and Wilderness Foundation Plymouth, Vermont
2012 – 2013	Watershed Policy Intern, Sonoran Institute Tucson, Arizona
2012 – 2013	Restoration Intern, Bureau of Land Management/ Southwest Conservation Corps Tucson, Arizona
2013	Farm Hand, Will Grow Organic Farm Anchor Point, Alaska

2014 – 2016	Research Assistant, Department of Fish, Wildlife, and Conservation Ecology. New Mexico State University Las Cruces, New Mexico
2015	Teaching Assistant, Department of Fish, Wildlife, and Conservation Ecology. New Mexico State University Las Cruces, New Mexico
2016	Teaching Assistant, Department of Geography. New Mexico State University Las Cruces, New Mexico
2016	Private Contractor, New Mexico Association of Conservation Districts Las Cruces, New Mexico
2017	Park Guide Trainee Pathways Intern, National Park Service White Sands National Monument, New Mexico

Professional and Honorary Societies

Phi Kappa Phi Honor Society

The Wildlife Society, New Mexico Student Chapter

Nivalis Conservation Network

American Association of University Women

Field of Study

Major Field 1: Applied Geography

Major Field 2: Fish, Wildlife, and Conservation Ecology

ABSTRACT

Three Neotropical species of nectar-feeding bats reach their northernmost extent in the southwestern United States. Plants of the genus *Agave* provide important nectar resources to these long-distance migrants, lesser long-nosed bats (*Leptonycteris yerbabuenae*), Mexican long-nosed bats (*Leptonycteris nivalis*), and Mexican long-tongued bats (*Choeronycteris mexicana*), throughout their ranges. Though regions with ample *Agave* may provide high quality habitat, no studies have explicitly modeled the distribution of *Agave* resources and strategically ground validated predictions. In this study, I utilize maximum entropy modeling (MaxEnt) to predict the distribution of an important summer resource, *Agave palmeri*, in the southwestern United States. I then ground validated the species distribution model in southwestern New Mexico and southern Arizona to test model accuracy and evaluate the reliability of commonly used presence threshold methods. In Chapter 1, I provide a technical background on the methods employed in this project, followed by a write up of the project in manuscript format in Chapter 2. I will discuss conservation implications and recommend topics for further study in Chapter 3. The results of this project indicate that distribution modeling for plants ought to be used as a biogeographical tool to inform more detailed studies, rather than as an indicator of species presence or absence. While model accuracy was low, using a predictive model to stratify field sites enhanced study efficiency. This study may indicate regions where restoration of *Agave* populations is warranted to enhance nectarivorous bat habitat.

TABLE OF CONTENTS

LIST OF TABLES

LIST OF FIGURES

INTRODUCTION

1.1 Introduction

In order to conserve and protect species, we must first know something about their distribution. In other words, where can we expect to find them and why? These questions can be answered in part by generating species distribution models. When modeling the distribution of species, researchers are confronted with the choice between presence-absence and presence-only methods. Presence-absence methods are often preferred in that they allow researchers to estimate detection probabilities of a species, yet there are many cases in which the collection of absence data may be infeasible, or when an abundance of presence records already exists. However, when using pre-existing records, such as museum or herbarium records, many biases may be incurred; data may not have been collected randomly, and spatial autocorrelation may be present. Taking these issues into account, Phillips et al. (2006) developed a method for modeling species distribution using presence-only data, known as maximum entropy modeling or MaxEnt.

In this project, I utilize MaxEnt to model the distribution of a patchy, non-clonal, long-lived, semelparous plant, *Agave palmeri* (Engelmann 1875), across its range in the southwestern United States. *Agave palmeri* is a paniculate agave of the subgenus *Agave* and Ditepalae Group (Gentry, 1982). This agave plant is an important nectar source for nectarivorous bats in the southwestern United States (Slauson, 1999; Ober and Steidl, 2004; Scott, 2004; England, 2012), and is the dominant summer food source in the only region in the United States where all three species of migratory nectarivorous bats are sympatric (Arita and Humphrey, 1988; Hoyt et al., 1994). In Figure 1.1, a map of confirmed occurrences for migratory nectarivorous bats in the southwestern United States is provided.

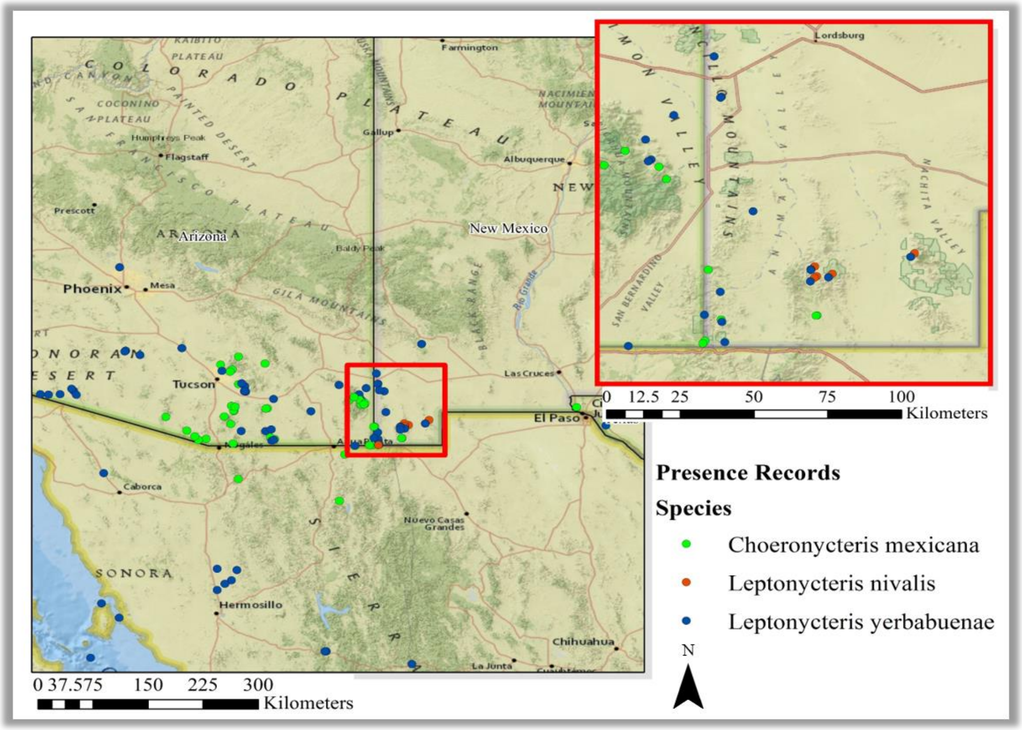

Figure 1.1 Confirmed presence records of migratory nectarivorous bats in the Southwestern United States

Due to the importance of *Agave* spp. in this portion of the range of nectarivorous bats, restoration and protection of *Agave* populations are recommended in recovery plans for both *Leptonycteris* spp. (USFWS, 1994; USFWS, 1995). However, few studies have investigated specific habitat requirements for *Agave* spp. in the southwestern United States. Additionally, no studies have explicitly modeled the distribution of *Agave* resources and strategically ground validated predictions. Taking these issues into account, the overall goals of this project are to determine the probability of presence of *A. palmeri* throughout the southwestern United States via a distribution model and to utilize this model to inform a ground-validation study to assess model accuracy and evaluate presence threshold methods. Because land managers have expressed interest in the distribution of *A. palmeri* to better understand the potential distribution of nectarivorous bats, I chose to employ a set of standard and repeatable methods to model the potential distribution of *A. palmeri* using a model selection approach.

I chose to utilize MaxEnt to meet the goals of this project for several reasons. First, *A. palmeri* exhibits a metapopulation structure in which many patches of plants occur across a wide range, and may be so isolated that patches can be considered subpopulations, relying on pollinators for functional connectivity (Gentry, 1982). These patches occur in rugged terrain, with accessibility limited by both natural features and land ownership status. Purely random surveys for this species have resulted in few detections (*S. Deeley, unpublished data*), and a predictive model with which to inform survey efforts was warranted to enhance study efficiency and effectiveness. Secondly, a multitude of presence records for *A. palmeri* were readily available from online herbaria databases, from a previous study conducted by a graduate student (*S. Deeley, unpublished data*), and from the local district botanist at the Las Cruces Bureau of Land Management District Office (*P. Alexander, unpublished data*). Each of these data sources presents various data collection biases, which can be effectively dealt with in MaxEnt (Phillips et al., 2006; Elith et al., 2011). The distribution model generated in MaxEnt informed a ground-validation study to see how well the model performed and to evaluate presence threshold methods. This study is part of a larger project assessing habitat suitability for nectarivorous bats throughout the southwestern United States.

In this introductory chapter, I will provide a more in depth background on MaxEnt and model selection methods employed in this project. In Chapter 2, I will present the methods and results of this study in manuscript format. In Chapter 3, I will discuss conservation implications of this project and recommend topics for further study. As a general conclusion, this study highlights the importance of considering species' reproductive biology when generating species distribution models and assessing their accuracy. Because plants have much more limited dispersal capabilities than animals, distribution modeling of plants may serve as a general biogeographical tool with which to inform further studies in which more detailed habitat associations are assessed. Nevertheless, distribution modeling may also effectively represent the metapopulation framework in which long-lived species colonize new patches and become extirpated from others, highlighting potentially important restoration areas. All in all, this study highlights the efficacy of using presence-only species distribution modeling to allocate survey efforts when studying patchy species with specific habitat preferences across a large range. This method for stratifying field surveys can help field researchers increase study efficiency, which is an important issue when dealing with the budgetary, staffing, and/or timeline restrictions with which many researchers are faced.

1.2 Species Distribution Modeling

When modeling the spatial dynamics of particularly rare, patchy, or elusive species, methods that allow researchers to estimate detection probabilities are often preferred. Integrating presence-absence data into an occupancy model is widely used in biological sciences, as this method can account for imperfect species detections (MacKenzie et al., 2002; Olson et al., 2005; MacKenzie et al., 2006; Nichols et al., 2008; Robinson et al., 2014). Despite the advantages of occupancy modeling, there are many instances in which the coordinated collection of presence-absence data across multiple sites is logistically infeasible. This is often the case for species with relatively large ranges or in remote tropical areas where biodiversity may be decreasing rapidly (Phillips et al., 2006).

When absence data is unavailable or unreliable, presence-only species distribution modeling can become a viable alternative. Species distribution modeling is used to predict a species' spatial relationships with both biotic and abiotic features on the landscape. Many biological researchers utilize multivariate analysis to understand relationships between species and landscape features (Gorressen et al., 2005) or tests of proportion between capture numbers and landscape features (Rojas-Martínez et al., 1999). These methods determine whether the strength of the association with features is greater or less than that which would be expected given random distribution. Traditional linear modeling methods are effective at revealing ecological relationships at various scales (Rojas-Martínez et al., 1999; Gorressen et al., 2005; Rainho and Palmeirin, 2011), yet may rely on the construction of directional hypothesis for species which we may know little about (Gorressen et al., 2005).

Presence-only models can be highly sensitive to sampling biases (Elith et al., 2011). Consequently, these methods are more appropriate for cases in which presence records have been collected systematically through formal biological surveys (Elith et al., 2011). It is for these reasons that traditional methods in presence-only modeling are unable to effectively utilize important sources of presence data, such as museum and herbarium collections (Elith et al., 2011). Software developed by Phillips et al. (2006), known as MaxEnt, helps reduce the biases associated with presence-only species distribution modeling by utilizing pseudo-absence data that is subject to the same biases as the input data (Phillips et al., 2006; Phillips et al., 2009). Furthermore, software that utilizes an information theoretic approach (*see section 1.3*) has since been developed to integrate model selection into MaxEnt, and additional data processing methods such as spatial filtering and species-specific tuning have been recommended in the literature to help further reduce model biases (Warren, 2010; Anderson and Gonzalez, 2011; Warren and Seifert, 2011; Boria et al., 2014; Warren et al., 2014).

Since its development, MaxEnt has been widely applied to species distribution modeling for flora and fauna alike. MaxEnt has been proven as an effective way to predict the distribution of species at multiple spatial and temporal scales (Razgour et al., 2011; Bellamy et al., 2013; Hayes et al., 2015), and performs well with relatively small sample sizes and multiple sources of input data (Frey et al., 2013; Van Proosdij et al., 2015). MaxEnt generates two probability densities, one from the landscape and one from the presence data, and minimizes the relative entropy between them (Elith et al., 2011). MaxEnt shows better discrimination between suitable and unsuitable areas for a species compared to another commonly used presence-only method, Genetic Algorithm for Rule-Set Prediction (Phillips et al., 2006). Moreover, MaxEnt is more effective at estimating species' realized distributions (Rebelo and Jones, 2010), and generates robust models with fairly small sample sizes, though the required sample size is dependent on the size of the species range (Van Proosdij et al., 2015).

MaxEnt models can be produced quickly, as data preparation is often the most time-consuming component of MaxEnt modeling (Young et al., 2011). The user-friendliness of MaxEnt, however, allows it to be easily misused. While MaxEnt provides a great contribution to conservation efforts, it is important to ensure it is used appropriately so as to not generate misleading or erroneous models. Ensuring that model inputs are biologically relevant and ensuring that the most relevant layers are utilized in the final model can help generate models that lead to effective conservation and management strategies. This can be achieved with a thorough literature review of the species being considered, an understanding of the statistics behind model selection and model validation, and appropriate data preparation and spatial filtering. Ground validation, a step that is often overlooked, can also help inform model accuracy (Searcy and Shaffer, 2014). Ground validation has the potential to lead to species detections in areas in which the species has not previously been documented (Rebelo and Jones, 2010), may provide a better method for statistical comparison of multiple models (Searcy and Shaffer, 2014), and can be used to evaluate threshold selection methods for determining probabilities at which a species is likely to be present in each grid cell (Nenzén and Araújo, 2011).

1.3 Model Selection with Presence-Only Models

Model selection in MaxEnt is typically based on the area under the receiver operating-characteristic curve (AUC), which can be defined as the probability that the model scores presence sites higher than absence sites (Phillips et al., 2009). The value of AUC ranges from 0 to 1, with a score closer to 1 indicating perfect discrimination between suitable and non-suitable sites, a score of 0.5 indicating random discrimination between suitable and non-suitable sites, and a score closer to 0 indicating less than random discrimination (Phillips et al., 2009). In the Figure 1.2, an example of the AUC curve using the species distribution model for *Agave palmeri* is provided. The black line represents an AUC value of .5, indicative of random predictive ability. Anything over the black line predicts species distribution at least better than random, while an AUC of 1 represents a model which perfectly represents reality.

AUC is the most commonly used metric for model selection in MaxEnt (Bellamy et al., 2013), but it may overestimate model accuracy or lead to the selection of overly complex models (Warren and Seifert, 2011; Searcy and Shaffer, 2014). Three forms of AUC that can be utilized in model selection include maximum training AUC, maximum test AUC, and minimum distance between training and test data. Maximum training AUC selects the model that maximizes AUC calculated from data that was used to create the model. Consequently, this is prone to selecting models that may over fit the data. Maximum test AUC uses test data that was withheld from the model construction to fit the best model. Minimum difference between training and test data helps to minimize the risk of over-parameterization, yet is reliant on a large sample size (Warren and Seifert, 2011).

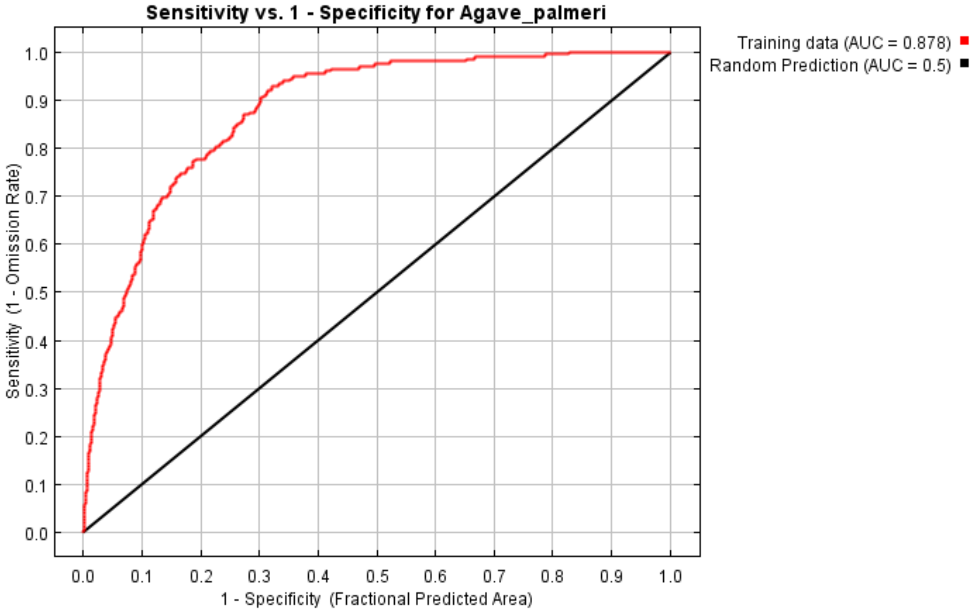

Figure 1.2 Area under the receiver operator characteristic curve (AUC) for *A. palmeri* distribution model

Model production in MaxEnt utilizes what is termed L_1 regularization, which minimizes the value of the equation in Figure 1.3 (Phillips et al, 2006). In the equation, the severity of the penalty term, β, is either accepted as the default setting or determined by the user (Warren and Seifert, 2011). This allows the user to determine how severely to punish additional and perhaps unnecessary parameters in the model so as to not over-fit the model. Determining how severely to penalize model complexity can be arbitrary. Additionally, as noted above, utilizing AUC as a model selection metric may lead to selecting models with more parameters (Warren and Seifert, 2011; Searcy and Shaffer, 2014). Information criterion metrics that utilize the principle of parsimony to penalize overly complex models may help avoid the issue of over parameterization and allow the regularization parameter in MaxEnt to be set non-arbitrarily.

$$\tilde{\pi}(-\ln[q_{\lambda}]) + \sum_{j} \beta_j|\lambda_j|$$

Figure 1.3 Maxent Equation. In this equation, the first term is the log loss, λ_j, while the second is the set of weights for the features upon which the model is built, along with a set of penalty terms, β_j (Phillips et al., 2006).

Information criterion approaches provide explicit criteria for penalizing model complexity and selecting the appropriate model (Warren and Seifert, 2011). One such method is using Akaike's Information Criterion (AIC), which utilizes maximum likelihood theory and the principal of parsimony to select the model that best fits the data without fitting an overly complex model (*see Figure 1.4;* Burnham and Andersen, 2002). Model selection using AIC is becoming widely accepted in ecological modeling (Johnson and Omland, 2004; Anderson, 2008). The use of AIC for competing models can help reveal complex ecological relationships that cannot be depicted with null hypothesis testing (Anderson, 2008).

$$\mathbf{AIC} = n\log(\hat{\sigma}^2) + 2K$$

$$\mathbf{AIC}_c = -2\log(\mathcal{L}(\hat{\theta})) + 2K\left(\frac{n}{n-K-1}\right)$$

Figure 1.4. Akaike’s Information Criterion (AIC) and Akaike’s Information Criterion adjusted for small sample size (AIC$_c$). Here, L is the maximum likelihood function, n is the sample size, and k is the number of parameters (Burnham and Andersen, 2002).

For spatial models, the program ENMTools (Warren et al., 2008; Warren et al., 2010) works in conjunction with MaxEnt by setting the regularization parameter according to that which achieves parsimony determined by an information criterion metric (Searcy and Shaffer, 2014; Warren et al., 2014). In a simulation study comparing model selection methods, Warren and Seifert (2011) found that AIC$_c$ (AIC adjusted for small sample size, *see Figure 1.4;* Burnham and Anderson, 2002) outperformed all AUC-based methods except for minimum AUC difference when sample size was 1000. Information criterion approaches to model selection may be significantly more useful when sample sizes are small (Warren and Seifert, 2011). However, it is important to note that information criteria are not a test, but rather a guideline for model selection that utilize non-arbitrary terms (Burnham and

Andersen, 2002). While it is important to take these considerations into account when choosing a method for model selection, it is also necessary to consider the potential benefits of ground-validating any model that was obtained using presence-only data.

1.4 Accuracy Assessment

Habitat distribution maps can be continually updated with new information, and are never truly a finished product (Boykin et al., 2007). Ground validation is an important part of this process, but this step in the modeling process is often overlooked. Ground validation presents the opportunity to detect species outside of previously surveyed areas and may effectively allocate survey efforts for rare or cryptic species (Rebelo and Jones, 2010; Searcy and Shaffer, 2014). Statistical measurements behind ground validation include omission, commission, the kappa statistic, and the true skill statistic (TSS). Omission errors can be defined as false absences, or the failure to predict that a species will exist in an area that it actually occupies. Commission is the opposite of omission in that it predicts a species will occupy an area that may actually be unsuitable (Rebelo and Jones, 2010). Distribution models generated for conservation guidelines may tend to err on the side of commission rather than omission errors (Boykin et al., 2007). The kappa statistic is a commonly used accuracy assessment metric, with a kappa value of 1 indicating perfect agreement between test data and model predictions, 0 indicating an agreement that is no better than random, and values closer to -1 indicating agreement that is worse than random (Allouche et al., 2006; Rebelo and Jones, 2010).

The kappa statistic is criticized for being prone to statistical artifacts based on species prevalence (Allouche et al. 2006), which can be defined as the percentage of a species range that is actually occupied (Van Proosdij et al., 2015). Allouche et al. (2006) show that another metric, the true skill statistic (TSS), does not produce the inherent biases of the kappa statistic, yet it retains the advantages of the kappa statistic. Figure 1.5 shows how each of these statistics is calculated based on an error matrix of omission and commission (Allouche et al., 2006). These metrics are each threshold dependent; a threshold from which to convert a continuous probability of occurrence surface into a binary presence-absence model must be established in order to obtain these metrics. The top of the figure shows an error matrix from which true presences (a), true absences (d), false presences (b), and false absences (c) can be determined using the ground validation dataset. The bottom portion of the figure shows how accuracy metrics can be calculated using a, b, c, and d.

1.5 Establishing a Presence Threshold

When generating species distribution models in which the output consists of a continuous probability surface with values ranging from 0 to 1, it is often necessary to convert these continuous values into a binary format to predict species presence or absence. Such is the case when estimating niche breadth, niche overlap, and niche contraction or expansion under climate change scenarios (Nenzén and Araújo, 2011), and when using threshold-dependent accuracy assessment metrics (Liu et al., 2011). However, converting a continuous probability surface into a binary format relies on determining threshold values which are often arbitrary and may even lack ecological basis (Liu et al., 2005; Warren et al., 2008; Nenzén and Araújo, 2011). Though determining these thresholds values can be problematic (Liu et al., 2005; Warren et al., 2008; Warren et al., 2010), accuracy assessment of distribution models is reliant on this presence threshold from which false presences, false absences, and accurate predictions can be determined.

<table>
<tr><th colspan="4"><i>Ground validation dataset</i></th></tr>
<tr><td colspan="2"></td><td>Presence</td><td>Absence</td></tr>
<tr><td rowspan="2"><i>Model</i></td><td>Presence</td><td>a</td><td>b</td></tr>
<tr><td>Absence</td><td>c</td><td>d</td></tr>
<tr><td colspan="4"></td></tr>
<tr><td colspan="2"><i>Measure</i></td><td colspan="2"><i>Formula</i></td></tr>
<tr><td colspan="2">Overall accuracy</td><td colspan="2">(a + d) / n</td></tr>
<tr><td colspan="2">Sensitivity</td><td colspan="2">a / (a + c)</td></tr>
<tr><td colspan="2">Specificity</td><td colspan="2">d / (b+ d)</td></tr>
<tr><td colspan="2">Kappa Statistic</td><td colspan="2">$\frac{([(a + d) / n)] - ((a + b)(a + c) + (c + d)(d + b))) / n^2}{1 - ((a + b)(a + c) + (c + d)(d +b))/ n^2}$</td></tr>
<tr><td colspan="2">TSS</td><td colspan="2">sensitivity + specificity - 1</td></tr>
</table>

Figure 1.5. Error matrix and formulae for accuracy assessment (adapted from Allouche et al., 2006). In each calculation, n = a + b + c + d.

The most commonly used method for presence-absence threshold selection, a fixed value approach (often fixed at 0.5) has been shown to perform the worst amongst other threshold section methods (Liu et al., 2005). In a model-based study, Liu et al. (2005) found that the best approaches were using a prevalence approach, average probability or suitability approach, sensitivity-specificity sum maximization approach, sensitivity-specificity equality approach, and a receiver operating characteristic curve (ROC) approach**.** In a later study, Liu et al. (2016) found that maximizing the sum of the sensitivity and specificity (MaxSSS) satisfies the criteria of objectivity, equality, and discriminability for threshold selection. This method has also been shown to perform well among multiple datasets (Liu et al., 2016). There are many factors to consider when selecting a threshold method, such as species reproductive biology, dispersal capabilities, and complexity of the distribution model from which predictions will be made. Due to disagreements in the literature regarding the best threshold methods, multiple threshold methods will be applied to the distribution model in this study, and an accuracy-assessment approach will be followed to select the best method based on a ground validation dataset.

1.6 Project Methods

Since the default regularization parameter ($\beta = 1$) in MaxEnt may have been tuned in a way that is not appropriate for all ecological systems and can lead to over-parameterization (Warren and Seifert, 2011; Warren et al., 2014), Warren et al. (2014) developed a standardized workflow from which to tune β, select variables based on percent contribution and correlation coefficients, and to re-tune β for the final variable set by utilizing AIC_c in either ENMTools or the MaxEnt Variable Selection Package in program R. In this project, I utilize these methods to establish a framework with which to model the distribution of *Agave palmeri* in the southwestern United States.

To generate this model, I integrated presence records for *A. palmeri* from the Global Biodiversity Information Facility (gbif.org), SEINet, from the Bureau of Land Management, Las Cruces District Office (*P. Alexander, unpublished data*), and from a previous study in southwestern New Mexico (*S. Deeley, unpublished data*). Using ENMTools (Warren et al., 2010), duplicate records were trimmed. Since multiple sources of presence records were utilized, and each had a different or unknown sampling methodology, I used the SDM Toolbox in ArcGIS 10.4.1 to rarefy occurrence records with a 1 km minimum distance filter to help mitigate issues of spatial autocorrelation (Boria et al., 2014). This brought the sample of 648 presence records down to a sample of 198. No presence records were withheld from the training data, since ground surveys would inform model accuracy.

Environmental layers in this model included 24 variables: 19 BioClim variables (Hijman et al., 2005), elevation (USGS, 2006), heat load (derived from elevation), soil (NRCS, 2016), geology (USGS 2005a; USGS 2005b), and land cover (USGS, 2004). The extent of the model was defined as the furthest 8-digit HUC watershed in which a presence record occurred. Because soil, geology, and land cover data was only available for the United States, the extent of this model was limited to the southwestern United States, and the range of *A. palmeri* in Mexico was not estimated, though artificially restricting the range of *A. palmeri* to the United States may impact model performance and ought to be investigated in the future. All layers were resampled to a resolution of 1 hectare so that the spatial resolution of the model would correspond with a sampling plot to be later used in the field.

Following model selection methods (Warren et al., 2014), I used all environmental variables to establish a preliminary set of 72 models in which each had a β value ranging from 0 to 15, adjusted in increments of 0.2. I selected the optimum value of β according to AIC_c in ENMTools (Warren et al., 2010; Warren and Seifert, 2011; Warren et al., 2014). I then discarded all environmental variables with less than 3 percent contribution to the optimum model. This contribution threshold was reduced from the 5 percent threshold utilized by Warren et al. (2014) because certain variables considered important to plant germination, establishment, and survival had a lower contribution when used with the whole suite of variables with which they may be highly correlated and 3 percent represented an integer value near the midpoint of 0 and 5 percent. Additionally, excessively pruning of model variables may overestimate niche breadth (Warren et al., 2014), and the goal of this study is to realistically model the distribution of *A. palmeri* to inform management decisions while also effectively and practically informing field sampling methodology.

After optimizing β for the final variable set, the most important variable according to that model was saved, and each variable following in importance was saved or discarded according to a correlation threshold. I used a correlation threshold of 70 percent for each variable in this study, as opposed to an 80 percent threshold used by Warren et al. (2014). Again, this was due to potential niche breadth overestimation with excessive model pruning. I then established a new suite of models using the final variable set to optimize β. The model with the optimum β value for the final set of variables then became the final model. All models generated following these methods utilized MaxEnt's raw output format, rather than the more commonly used logistic output, due to issues of model comparison and assumptions regarding species' prevalence when comparing scaled models (Merow et al., 2013). However, after selecting the top model, I used the same β value and final variable set from the top model to generate a model in the logistic output format in order to easily stratify ground validation field sites across a range of probabilities of occurrence. Since the highest predicted probability of occurrence in the top model in a given cell was 94.35 percent, the model was reclassified into 5 classes using equal intervals in ArcGIS 10.4.1, as opposed to fixed intervals between 0 and 100 percent. These classes were used to stratify accuracy assessment sites to ensure adequate representation of the whole range of probabilities of occurrence throughout the study area and are defined in Table 1.1.

Table 1.1. Stratification Class Definitions

Class	***Probability of Occurrence***
1	0 - 19.38
2	19.38 - 38.12
3	38.12 - 56.87
4	56.87 - 75.61
5	75.61 – 94.35

Using ArcGIS 10.4, I extracted the reclassified raster by road buffers of 1 km, 0.5 km, and by an area of interest comprised of southeastern Arizona and southwestern New Mexico, and intersected it with a layer of federal land derived from the Protected Areas Database (USGS, 2016). I then converted this extracted area to point, with each point corresponding with the center of a 1-hectare pixel. I then used the sampling design tool (Buja and Menza, 2013) in ArcGIS 10.4.1 to select a random sample of points stratified by suitability class, with a minimum distance of 5 km between points. Two hundred and fifty points within 1 km from the road were selected, and 250 points within .5 km from the road were selected, totaling 500 survey points and 100 points in each class. Road buffers allowed field survey sites to be accessed quickly while also representing various distances from road features so as to not over-represent disturbed habitats.

Although land status was accounted for when selecting survey points, previous surveys in the summer of 2015 informed me that access issues would still be encountered. Therefore, I set a goal of reaching 250 of these points during the summer of 2016. Because each point corresponded with the center of a pixel, each pixel corresponded with a probability of occurrence according to the model, and the project goal was to determine if the model could predict *A. palmeri* presence or absence, each point became the center of a survey plot, with the plot size corresponding with the size of the pixel. Points were located on the landscape using a Garmin Rino 610. I conducted all surveys on land managed by the Bureau of Land Management, U.S. Forest Service Coronado District, or U.S. Fish and Wildlife Service(Special Use Permit # 015-2016).

Within each survey plot, I established the base of the plot by walking 50 m from the center point, due north or south if the plot was flat, or adjusted based on the contour if the plot was on a hillside. Then, I ran a 100 m transect tape along the base of the plot, and walked parallel 100 m x 5 m belt transects at the 80 m, 60 m, 40 m, and 20 m marks on the base. Figure 1.6 shows a conceptualized diagram of these methods in a 100 m by 100 m plot. Figures 1.7a and 1.7b show an example of these methods in various habitat types, with the focal species visible in the right foreground of Figure 1.7a, and in the horizon of Figure 1.7b.

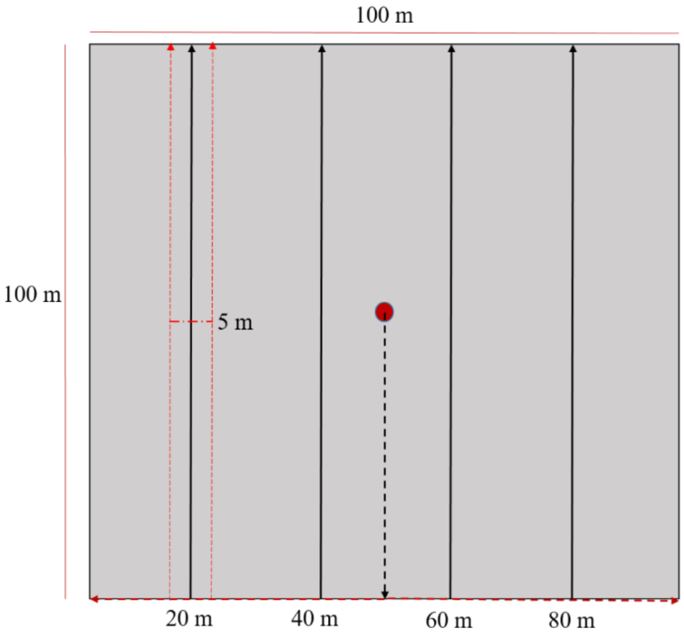

Figure 1.6 Survey methods in 1 hectare plot (gray square). Red dot is plot center, and black dashed arrow is path walked to establish plot base, represented by red dashed arrows at bottom of square. Solid black arrows represent belt transects walked, with parallel red dashed arrows representing belt transect width.

These survey methods resulted in surveying 20 percent of each plot and pixel. Within each belt transect, I counted the number of *A. palmeri* or determined the absence of the species. A set of rules was established to preclude running transects in areas where it was evident that no *A. palmeri* was present. If an area was flat, had over 80 percent bare ground, no visual obstructions, and no *A. palmeri* visible on the surrounding landscape from the plot center, I determined that *A. palmeri* was absent from the plot and did not conduct transects. This was often the case in sparse lowland habitats dominated by creosote bush (*Larrea tridentata*) or in dry playa lakebeds. Figure 1.8 shows an example of a site that meets these criteria. In other instances, it was clear that *A. palmeri* was present in a plot, yet natural barriers such as cliffs, or artificial barriers such as mine shafts, prevented the establishment of transects. In these instances, *A. palmeri* was determined to be present but a count was not obtained.

Figure 1.7a. (Left) Belt transects in Quercus/Juniperus/Arctostaphylos scrub

Figure 1.7b. (Right) Belt transects in Larrea tridentata desert scrub

Figure 1.8 Barren site that meets criteria to determine absence of A. palmeri without running belt transects

The ground validation dataset obtained using these methods allowed me to assess model accuracy based on multiple presence threshold methods easily applied via the graphical user interface MaxEnt. Seven threshold methods were considered, which can be seen in the Table 1.2. Each threshold was applied to the logistic output of the final *A. palmeri* model using MaxEnt, except for the Fixed50 method, which was applied using ArcGIS.

Thresholds were used to determine predicted presence or absence according to the model, and the ground validation dataset was used to assess threshold accuracy and select the best method. When compared to the ground validation dataset, these predictions allowed for the determination of the overall accuracy, sensitivity, specificity, kappa statistic, and true skill statistic (Allouche et al., 2006). Each of these threshold methods was applied to determine the best threshold method for *A.*

palmeri based on the true skill statistic, which represents the true positive rate minus the false negative rate (Freeman and Moisen, 2008). However, commission error (low specificity) may be acceptable in a distribution model with goals of informing potential restoration sites. While ground validation may indicate a species is not present in a given area in which it was predicted to occur, this may be due to external issues such as habitat disturbance or even illegal harvesting, rather than species habitat preferences. These areas should not necessarily be dismissed as unsuitable habitat when assessing species distribution model accuracy and may be effective restoration areas if they are since free of disturbing factors.

Table 1.2. Threshold Methods, Abbreviations, and Values

Presence Threshold Method	***Abbreviation***	***Threshold Value***
Balance Training Omission, Predicted Area, and Threshold Value	BOAT	0.098
Equate Entropy of Thresholded and Original Distribution	EETOD	0.159
Equal Training Sensitivity and Specificity	ETSS	0.312
Fixed Threshold Value of 0.50	Fixed50	0.500
Maximum Training Sensitivity plus Specificity	MaxSSS	0.191
Minimum Training Presence	MTP	0.032
10 Percentile Training Presence	10Per	0.210

In the following chapter, I layout this project in manuscript format, focusing on the distribution and binary models generated for *A. palmeri* and the results of ground validation. The paper will be submitted to *The Journal of Arid Environments*. I hope this project provides important information to land managers by setting the stage for site prioritization for habitat improvement projects, leading to effective habitat management strategies for both *A. palmeri* and nectarivorous bats.

CHAPTER 2.

Modeling the Distribution of Palmer's Agave (Agave palmeri) throughout the Sympatric Summer Ranges of Nectarivorous Bats (Phyllostomidae: Glossophaginae) using Presence-only Species Distribution Modeling

To Be Submitted To:

The Journal of Arid Environments

Rachel A. Burke, Christopher Brown, Kathryn E. Stoner, Carol Campbell

ABSTRACT

Nectarivorous bats in the southwestern United States, two of which are federally endangered, are reliant on nectar from plants of the genus *Agave* to meet energy needs during the summer and early fall, prior to seasonal migration. Restoration and protection of *Agave* populations have been recommended in recovery plans for endangered nectarivorous bats, yet few studies have investigated specific habitat requirements for *Agave* spp. in the southwestern United States. Though areas with ample agave resources indicate high habitat quality for nectarivorous bats, no studies have explicitly modeled the distribution of *Agave* spp. and strategically ground validated predictions. In this study, we utilize maximum entropy modeling (MaxEnt) to predict the distribution of an important summer resource, *Agave palmeri,* in sympatric summer ranges for nectarivorous bats in the southwestern United States, following a standardized model selection approach. We then ground validated the model to test its accuracy and to evaluate presence threshold methods. High sensitivity and low specificity of each threshold method indicate the model may be better at indicating potential habitat rather than actual species presence for *A. palmeri*, yet model accuracy appeared to be higher in certain regions than in others. *Agave palmeri* was present at every site surveyed in the Chiricahua Mountains, indicating that this region can provide high quality habitat for nectarivorous bats throughout the flowering period of *A. palmeri*. Regions where *A. palmeri* was predicted to be present yet the species did not occur may highlight areas where restoration of *A. palmeri* is warranted.

1. Introduction

Three Neotropical species of nectar-feeding bats (Phyllostomidae: Glossophaginae) reach their northernmost extent in the southwestern United States. These long-distance migrants, lesser long-nosed bats (*Leptonycteris yerbabuenae*), Mexican long-nosed bats (*Leptonycteris nivalis*), and Mexican long-tongued bats (*Choeronycteris mexicana*), play important ecological roles by pollinating their food resources, dispersing seed of columnar cacti, and reducing genetic isolation in their food resources (Howell and Roth, 1981; Horner et al., 1998; Godinez-Alvarez and Valiene-Banuet, 2000; Rocha et al., 2006; Fleming et al., 2009; Rojas-Martínez et al., 2012). While the southernmost populations of these species may not undergo long-distance latitudinal migrations because of year-round food availability (Rojas-Martínez et al., 1999; Stoner et. al., 2003; Rojas-Martínez et al., 2012; Cajas-Castillo et al., 2015;), their northern counterparts migrate along a nectar corridor of columnar cacti and *Agave* species throughout the Chihuahuan and Sonoran Deserts (Wilkinson and Fleming, 1996; Fleming et al., 1993). Two species of nectarivorous bats in the United States are federally endangered (*Leptonycteris nivalis, L. yerbabuenae*); restoration and protection of *Agave* populations have been recommended in recovery plans for both (USFWS, 1994; USFWS, 1995).

In the only regions in the United States where all three species of nectarivorous bats are sympatric (Arita and Humphrey, 1988; Hoyt et al., 1994), nectar from *Agave* spp. becomes the dominant food source. Palmer's agave (*Agave palmeri*; Engelmann 1875), a monocarpic, semelparous, paniculate agave of the subgenus *Agave* and Ditepalae Group (Gentry, 1982), provides an important resource for nectarivorous bats in this region (Slauson, 1999; Ober and Steidl, 2004; Scott, 2004; England, 2012). Despite the need to better understand habitat requirements of *Agave* spp. in order to better understand the potential distribution of nectarivorous bats, few studies have investigated specific habitat requirements for *Agave* spp. in the southwestern United States.

The overall goal of this study is to obtain information that will help inform management and restoration of *A. palmeri* populations throughout the southwestern United States and consequently assist in the conservation of nectarivorous bats in this region. The specific objectives are to:

1) Generate a species distribution model (SDM) of *A. palmeri* to determine the probability of presence throughout the southwestern United States.

2) Utilize this SDM to inform a ground-validation study to assess model accuracy.

3) Select the optimal presence threshold method based on the ground validation dataset to delineate the range of *A. palmeri* to inform restoration plans and to recognize potential high quality resource areas for nectarivorous bats.

2. Methods

2.1 Methods Background

A presence-only approach was followed to meet the modeling goals of this project. Upon reviewing presence-only methods, maximum entropy modeling

(MaxEnt: Phillips et al., 2006) was selected for several reasons. *Agave palmeri* exhibits a metapopulation structure in which many patches of plants occur across a wide range (Gentry, 1982). These patches occur in rugged terrain, with accessibility limited by both natural features and land ownership status. Purely random surveys for this species have resulted in few detections (*S. Deeley, unpublished data*), warranting the use of a predictive model with which to stratify field studies.

MaxEnt is a viable choice to generate this predictive model. MaxEnt shows better discrimination between suitable and unsuitable areas for a species compared to other commonly used presence-only methods (Phillips et al., 2006), may be more effective at estimating species' realized distributions (Rebelo and Jones, 2010), and generates robust models with fairly small sample sizes (Van Proosdij et al., 2015). Furthermore, a multitude of presence records for *A. palmeri* is readily available from multiple data sources. Each source contains various and unknown data collection biases, making traditional linear modeling inappropriate (Elith et al., 2011). MaxEnt helps reduce the biases associated with presence-only species distribution modeling by utilizing pseudo-absence data that is subject to the same biases as the input data and is thus able to utilize various sources of presence records that were not necessarily collected systematically (Phillips et al., 2006; Phillips et al., 2009; Elith et al., 2011).

To select parsimonious models that will remain relevant in novel environments and shifting climatic scenarios, software has been developed to integrate model selection into MaxEnt (Warren, 2010; Warren and Seifert, 2011;

Warren et al., 2014). The program ENMTools (Warren et al., 2008; Warren et al., 2010) works in conjunction with MaxEnt by allowing the user to compare multiple models in which the regularization parameter in MaxEnt is adjusted and input variables are removed or retained according to a correlation threshold (Warren et al., 2014). These multiple models are then compared; the optimal model can be selected based on an information criterion metric that utilizes the principle of parsimony to penalize overly complex models, including Akaike's Information Criterion (AIC), Akaike's Information Criterion Adjusted for Small Samples (AIC_c), and Bayesian Information Criterion (BIC) (Burnham and Anderson, 2002; Warren et al, 2008; Warren et al., 2010). Models selected according to a more commonly used metric, the area under the receiver operating characteristic curve (AUC), are often over-parameterized (Warren and Seifert, 2011; Searcy and Shaffer, 2014).

Models produced in MaxEnt generate an output of a continuous probability surface in which the relative occurrence rate (ROR) in each grid cell reflects a species' likelihood of presence relative to other cells; this value can be left in raw format or logistically transformed (Merow et al., 2013; Merow et al., 2016). It is useful to convert these continuous values into a binary format to predict species presence or absence when estimating species niche breadth, niche overlap, and niche contraction or expansion under climate change scenarios (Nenzén and Araújo, 2011), and when using threshold-dependent accuracy assessment metric (Freeman and Moisen, 2008). Though converting a continuous probability surface into a binary format relies on determining threshold values which are often arbitrary (Liu et al., 2005; Warren et al., 2008; Nenzén and Araújo, 2011), accuracy assessment of distribution models is reliant on this presence threshold to determine sensitivity and specificity of the model.

Recent studies suggest that maximizing the sum of the sensitivity and specificity (MaxSSS) is the best method in threshold selection, while the most commonly used method, a fixed value of 0.5, has been shown to perform the worst (Liu et al., 2005; Liu et al., 2016). Threshold selection can also follow an accuracy assessment approach in which a ground validation dataset is used to determine the best threshold method (Nenzén and Araújo, 2011). Due to disagreements in the literature regarding the best threshold methods, we follow an accuracy assessment approach in this study. The best threshold method will be selected based on that which performs the best according to a ground validation dataset, which we obtain via field surveys for *A. palmeri*.

2.2 Species Distribution Modeling for A. palmeri

Presence records in this model were obtained from multiple sources, including the Global Biodiversity Information Facility (gbif.org), SEINet, from the Bureau of Land Management, Las Cruces District Office (*P. Alexander, personal communication*), and from a previous study in southwestern New Mexico (*S. Deeley, personal communication*). Using ENMTools (Warren et al., 2010), all duplicate records were trimmed. Since multiple sources of presence records were utilized, and each had a different or unknown sampling methodology, we used the SDM Toolbox in ArcGIS 10.4.1 to rarefy occurrence records with a 1 km minimum distance filter to help mitigate issues of spatial autocorrelation (Boria et al., 2014). This brought the sample of 648 presence records down to a sample of 198. No presence records were withheld from the training data for testing.

Environmental layers in this model included 24 variables: 19 BioClim variables (*see Table 2.1 for definitions*; Hijmans et al., 2005), elevation (USGS, 2004), heat load (derived from elevation), soil (NRCS, 2016), geology (USGS 2005a; USGS 2005b), and land cover (USGS, 2004). We defined the extent of the model based on the furthest 8-digit watershed unit in which a presence record occurred. Because soil, geology, and land cover data were only available for the United States, the extent of this model was limited to the southwestern United States, and the range of *A. palmeri* in Mexico was not estimated, though the influence of this artificial range boundary ought to be investigated in the future. All layers were resampled to a resolution of 1 hectare so that the spatial resolution of the model would correspond with a sampling plot used in the field.

Table 2.1
BioClim Variable Definitions (Hijmans et al., 2005)

BioVar	***Definition***
Bio 1	Annual Mean Temperature
Bio 2	Mean Diurnal Range (Mean of monthly (max temp-min temp)
Bio 3	Isothermality (BIO2/BIO7) (* 100)
Bio 4	Temperature Seasonality (standard deviation *100)
Bio 5	Max Temperature of Warmest Month
Bio 6	Min Temperature of Coldest Month
Bio 7	Temperature Annual Range (BIO5-BIO6)
Bio 8	Mean Temperature of Wettest Quarter

Bio 9	Mean Temperature of Driest Quarter
Bio 10	Mean Temperature of Warmest Quarter
Bio 11	Mean Temperature of Coldest Quarter
Bio 12	Annual Precipitation
Bio 13	Precipitation of Wettest Month
Bio 14	Precipitation of Driest Month
Bio 15	Precipitation Seasonality (Coefficient of Variation)
Bio 16	Precipitation of Wettest Quarter
Bio 17	Precipitation of Driest Quarter
Bio 18	Precipitation of Warmest Quarter
Bio 19	Precipitation of Coldest Quarter

Following model selection methods outlined by Warren et al. (2014), we used all environmental variables to establish a preliminary set of 72 models in which each had a β value ranging from 0 to 15, adjusted in increments of 0.2. We selected the optimum value of β according to AIC$_c$ (Akaike's Information Criterion adjusted for small sample size) in ENMTools (Warren et al., 2010; Warren and Seifert, 2011; Warren et al., 2014). All environmental variables with less than 3 percent contribution to the optimum model were discarded. This contribution threshold was reduced from the 5 percent threshold utilized by Warren et al. (2014) because certain variables considered important to plant germination, establishment, and survival had a lower contribution when used with the whole suite of variables with which they may be highly correlated, and 3 represents an integer value near the midpoint of 0 and 5 percent. Additionally, excessive pruning of model variables may overestimate niche breadth (Warren et al., 2014).

After optimizing β for the final variable set, we saved the most important variable according to that model, and saved or discarded each variable following in importance according to a correlation threshold. A correlation threshold of 70 percent was used for each variable in this study, as opposed to an 80 percent threshold used by Warren et al. (2014). Again, this was due to potential niche breadth overestimation with excessive model pruning. We then established a new suite of models to optimize β for the final set of variables. The model with the optimum β value for the final set of variables according to AIC_c then became the final model.

2.3 Presence/Absence Thresholds

Seven threshold methods were applied to the final *A. palmeri* model to generate a binary map indicating predicted presence or absence of *A. palmeri* (Table 2.2). Each of these threshold methods can be easily applied to a continuous distribution model via the graphical user interface in MaxEnt, except for the Fixed50 method, which is easily applied using the reclassify tool in ArcGIS. In order to select the best threshold method, a ground validation dataset obtained from field surveys was utilized (*see section 2.4*).

Table 2.2
Presence thresholds for *A. palmeri*

Presence Threshold Method	***Abbreviation***	***Threshold Value***
Balance Training Omission, Predicted Area, and Threshold Value	BOAT	0.098
Equate Entropy of Thresholded and Original Distribution	EETOD	0.159
Equal Training Sensitivity and Specificity	ETSS	0.312
Fixed Threshold Value of 0.50	Fixed50	0.500

Maximum Training Sensitivity plus Specificity	MaxSSS	0.191
Minimum Training Presence	MTP	0.032
10 Percentile Training Presence	10Per	0.210

2.4 Field Site Selection and Surveys

When establishing initial models, we used MaxEnt’s raw output format, rather than the more commonly used logistic output, due to issues with model comparison and assumptions regarding species’ prevalence when using scaled models (Merow et al., 2013). However, after selecting the top model, we applied the same β value and final variable set from the top model to generate a model in the logistic output format in order to stratify ground validation field sites across a range of probabilities of occurrence. We reclassified this model for *A. palmeri* into 5 classes using equal intervals in ArcGIS 10.4.1, corresponding with ranges in probability of occurrence.

Using ArcGIS 10.4.1, we extracted the reclassified raster by road buffers of 1 km, 0.5 km, by an area of interest comprised of southern Arizona and southwestern New Mexico, and intersected it with a layer of federal land derived from the Protected Areas Data Portal (USGS, 2016). We converted the extracted raster to point, with each point corresponding with the center of a 1-hectare pixel, and used the sampling design tool (Buja and Menza, 2013) to select a random subset of points stratified by suitability class, with a minimum distance of 5 km between points. Two hundred and fifty points within 1 km from the road were selected, and 250 points within 0.5 km from the road were selected, totaling 500 survey points and 100 points in each class. Road buffers allowed field surveys to be accessed quickly while also representing various distances from road features so as to not over-represent disturbed habitats. Although land status was accounted for when selecting survey points, previous surveys in the summer of 2015 indicated that access issues would still be encountered. Therefore, we set a goal of reaching 250 of these points, with 50 points in each of the 5 classes to ensure adequate coverage across the whole range of probabilities.

To conduct field surveys, each point became the center of a survey plot, with the plot size corresponding with the size of the pixel. We located points on the landscape using a Garmin Rino 610. We conducted all surveys on land managed by the Bureau of Land Management, U.S. Forest Service, or U.S. Fish and Wildlife Service (Special Use Permit # 015-2016). Within each survey plot, we established the base of the plot by walking 50 m from the center point, due north or south if the plot was flat, or adjusted based on the contour if the plot was on a hillside. We placed a 100 m transect tape along the base of the plot and walked 4 parallel 100 m x 5 m belt transects from the base (Figure 2.1).

Within each transect, we counted the number of *A. palmeri* or determined the absence of the species. We established a set of rules to preclude running transects in areas where it was evident that no *A. palmeri* was present. If an area was flat, had over 80 percent bare ground, no visual obstructions, and no *A. palmeri* visible on the surrounding landscape from the plot center, we considered *A. palmeri* to be absent from the plot and transects were not conducted. In other instances, it was clear that *A. palmeri* was present in a plot, yet natural or artificial barriers prevented the establishment of transects. In these instances, we determined *A. palmeri* to be present, but we did not obtain a count.

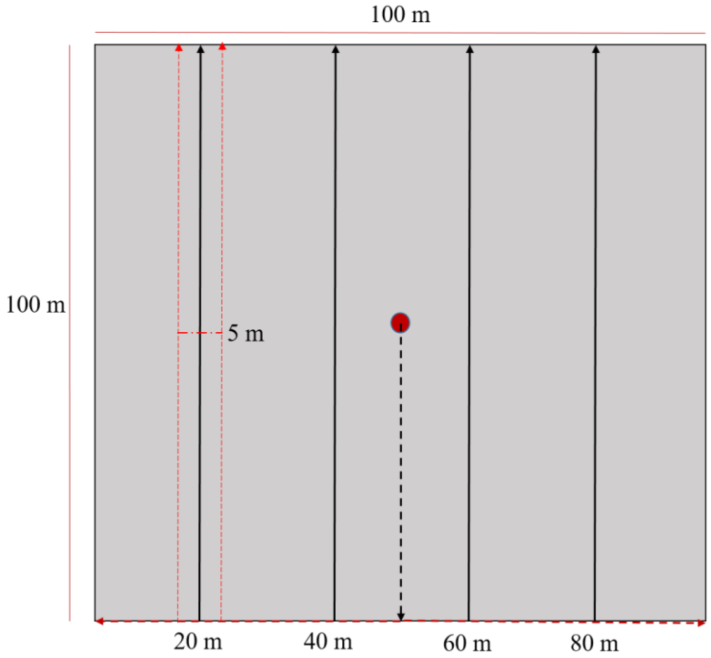

Figure 2.1 Survey methods in 1 hectare plot (gray square). Red dot is plot center, and black dashed arrow is path walked to establish plot base, represented by red dashed arrows at bottom of square. Solid black arrows represent belt transects walked, with parallel red dashed arrows representing belt transect width.

Using ArcGIS 10.4.1, we compared the ground validation dataset obtained using these methods to areas of predicted presence and predicted absence according to each threshold method. Total numbers of accurately predicted presences, accurately predicted absences, and total numbers of false presences and false absences were determined for each threshold method. These values allowed for the determination of the overall accuracy, sensitivity, specificity, kappa statistic, and true skill statistic (TSS), as defined in Allouche et al. (2006). The best presence/absence threshold method was selected according to the TSS.

3. Results

3.1 Agave palmeri species distribution model

In the model selection process, 72 preliminary distribution models of *A. palmeri* were generated, in which each had a β value between 0 and 15, adjusted in increments of 0.2. Using ENMTools, we optimized β for the preliminary model at β = 6.0 according to AIC_c. Variables with over 3 percent contribution to this preliminary model included Bio 18, Bio 9, Bio 11, Bio 13, Bio 15, Bio 1, Bio 6, Bio 7, Bio 8, soil, and Bio 5. Variables were saved or discarded in order of importance according to the correlation threshold, leaving Bio 18, Bio 7, Bio 15, Bio 9, Bio 11, Soil, Bio 5, Bio 1, and Bio 8 in the final variable set. Using the final variable set, we retuned β to an optimal value of β = 4.2. Variable contributions for this model can be seen in Table 3.1. The final model is shown in Figure 3.1, presented in logistic format for ease of interpretability, along with the 198 spatially rarefied presence records used to train the model.

Table 3.1
Variable importance for final *A. palmeri* model (β = 4.2)

Variable	*Percent Contribution*	*Permutation Importance*
Bio 18	23.4	47.7
Bio 7	21.4	3.1
Bio 15	19.3	3.4

Bio 9	18.7	25.1
Bio 11	9.6	3.4
Soil	6.3	4.6
Bio 5	1.2	6.8
Bio 1	0.2	6
Bio 8	0	0

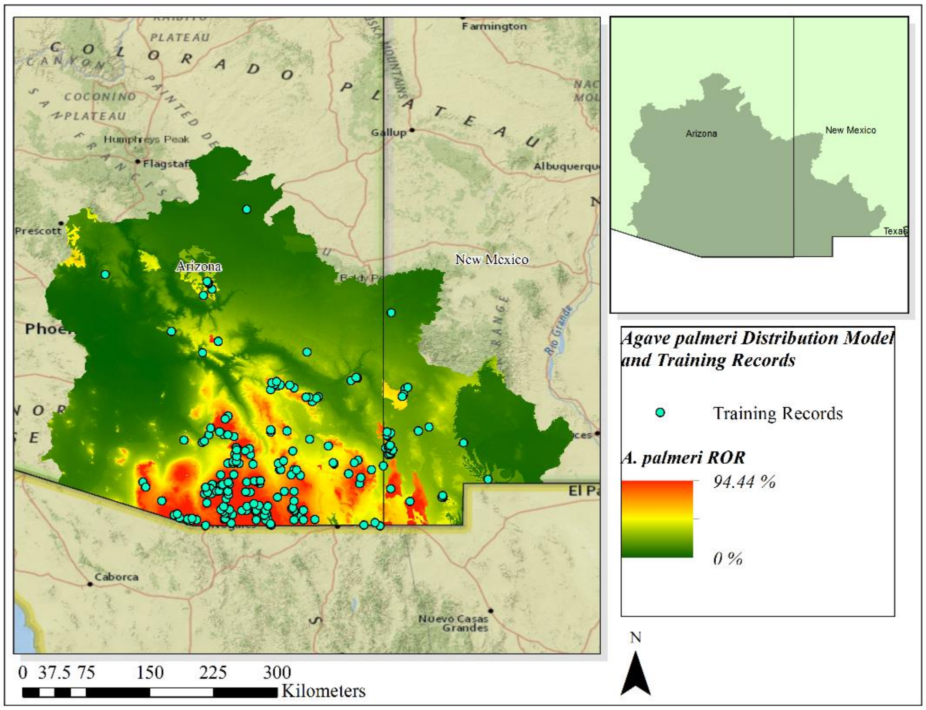

Figure 3.1 Top *A. palmeri* distribution model and training records, logistic output.

3.2 Field Surveys and Threshold Testing

Between June and October of 2016, we surveyed 115 sites. This fell short of the goal of 250 sites, as we encountered many access issues throughout the season. We detected *A. palmeri* at 33.04 percent of sites (n = 38), and determined *A. palmeri* to be absent from 66.96 percent of sites (n = 77). Surveys fell primarily within the

Animas, Big Burro, Chiricahua, Huachuca, Mule, Patagonia, Peloncillo, Pinaleño, and Santa Catalina Mountain Ranges, as well as in intermittent valleys.

3.3 Threshold Selection and Predicted Range

We established seven binary maps indicative of predicted presence or absence by applying various threshold methods to the continuous *A. palmeri* distribution model, which were outlined in Table 2.2. These maps can each be seen in Figure 3.2. We selected the best model according to TSS, which we calculated using the ground validation dataset. The selected threshold can be seen in more detail in Figure 3.3, along with the ground validation dataset survey locations.

Each of the presence threshold methods had a high sensitivity and was effectively able to predict species presence. However, high sensitivity came at the expense of low specificity. Inaccurately predicted presences were common amongst all methods (n = 62.86 ± 8.68). While the fixed threshold method had the highest overall accuracy, the threshold method which maximized TSS, ETSS, was ultimately chosen. The equal training sensitivity and specificity method also maximized kappa, had the second highest specificity, and second highest overall accuracy (Table 3.2). The worst performing metric was the minimum training presence, which predicted the presence of *A. palmeri* throughout almost the entire study area (82.2 percent). The selected threshold method, ETSS, predicted *A. palmeri* presence throughout 21.2 percent of the study area. Model accuracy appeared to fluctuate throughout the study area. *Agave palmeri* was present in every site surveyed in the Chiricahua Mountains, with highly variable total counts. Fluctuations in *A. palmeri* density (28.88 ±100.77 ha^{-1}) across the study area will be assessed in a future study.

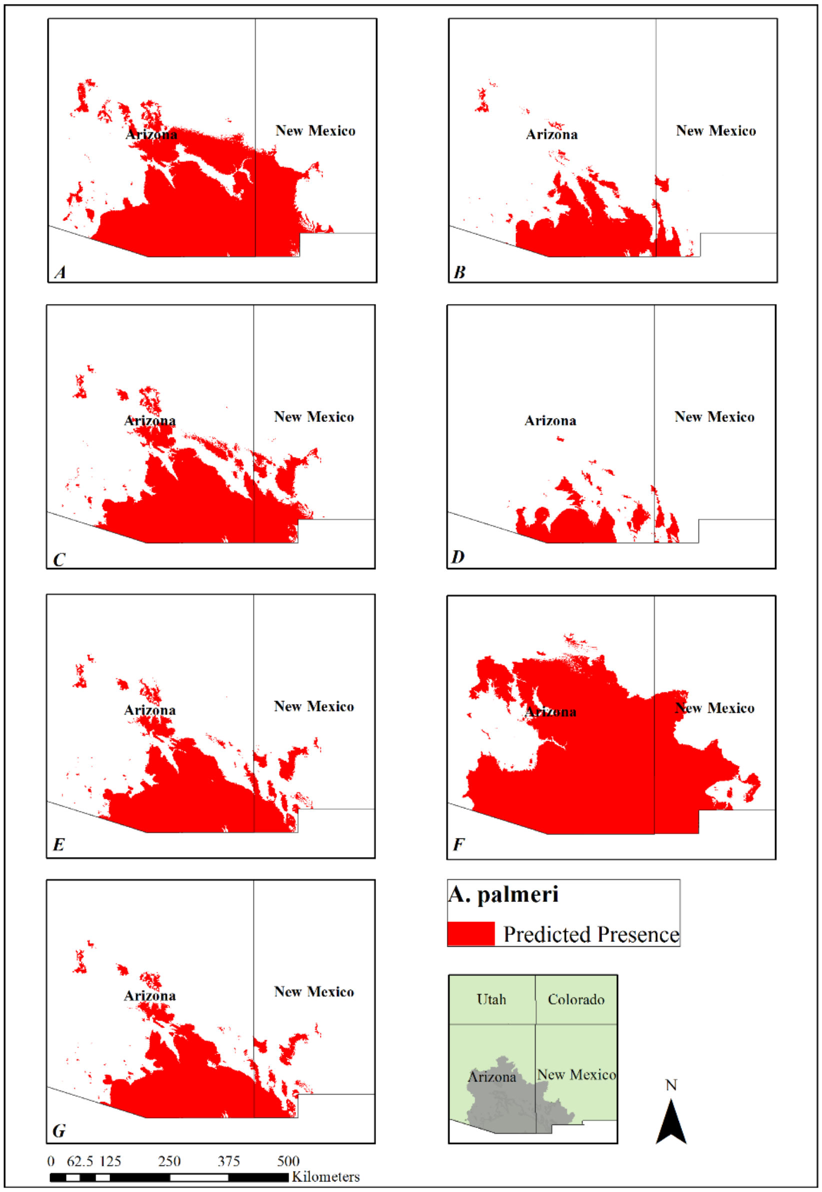

Figure 3.2 Presence thresholds, *A. palmeri.* A = BOAT, B= EETOD, C = ETSS, D = Fixed50, E = MaxSSS, F = MTP, G = 10Per (*see Table 2.2 for abbreviation definitions*).

Table 3.2

Accuracy assessment metrics based on ground validation dataset and fractional predicted area for each (shown in order of decreasing TSS)

Threshold Method	*Overall Accuracy*	*Sensitivity*	*Specificity*	*Kappa*	*TSS*	*Predicted Area*
ETSS	0.5043	0.8947	0.3117	0.1556	0.2064	21.2 %
10Per	0.4783	0.9474	0.2468	0.1414	0.1941	30.2 %
Fixed50	0.5130	0.8421	0.3506	0.1490	0.1928	10.0 %
MaxSSS	0.4261	1.0000	0.1429	0.0992	0.1429	32.2 %
EETOD	0.4174	1.0000	0.1299	0.0898	0.1299	38.4 %
BOAT	0.3826	1.0000	0.0779	0.0529	0.0779	52.2 %
MTP	0.3478	1.0000	0.0260	0.0173	0.0260	82.8 %

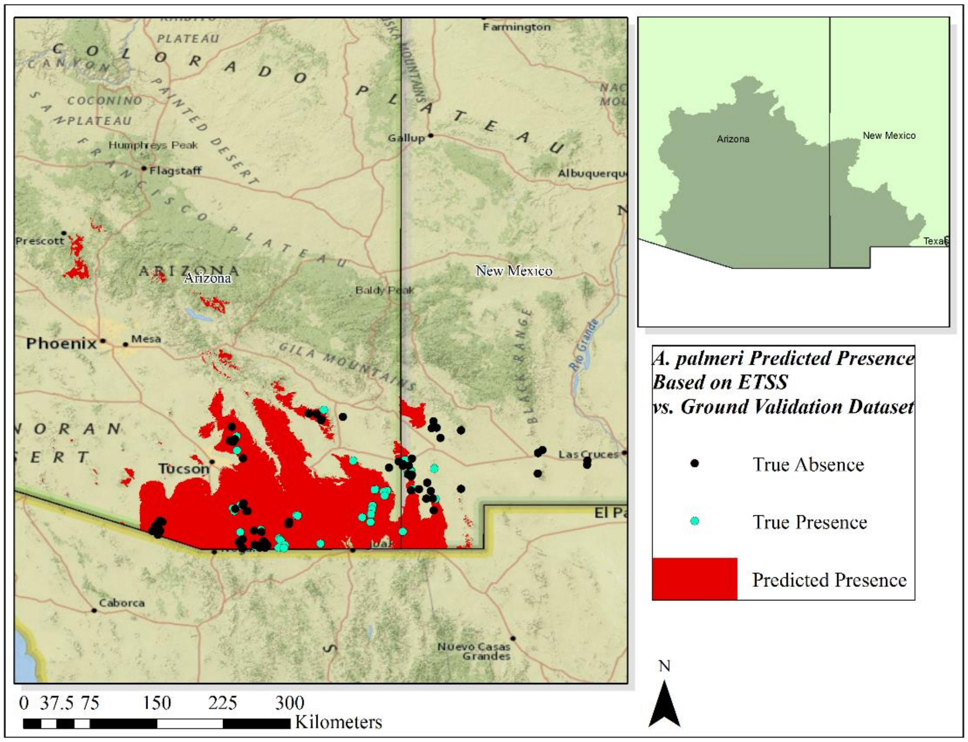

Figure 3.3 Predicted presence and absence of A. palmeri based on the ETSS threshold method vs. actual presence and absence based on the ground validation dataset. NAD 1983, Zone 12.

4. Discussion

We verified the true presence of *A. palmeri* throughout the study region, and detected the highest numbers of individual plants in the Chiricahua, Dos Cabezas, and southern Peloncillo Mountains. While the Chiricahua Mountains have been extensively studied, little research has taken place in the southern Peloncillo Mountains, largely due to access issues. We also detected *A. palmeri* in the Pyramid Mountains of New Mexico, both in survey plots and incidentally throughout the region. Given the prevalence of abandoned mines in this region, further surveys for nectarivorous bats in the region are warranted. Collaboration with private landowners in the region is also warranted, as many large patches of *A. palmeri* were incidentally observed to fall on private lands, and abandoned mines within foraging distance from these patches also appeared to fall within private lands. This would help us not only to better understand the distribution of *A. palmeri*, but also would help identify potential habitat for species that rely on *Agave* nectar to meet their energy needs, particularly endangered *Leptonycteris*.

Overall, the detection of *A. palmeri* at 33.04 percent of survey sites was a significant improvement from detections in a previous preliminary unstratified study in which we detected *A. palmeri* at 2.16 percent of sites (*S. Deeley, personal communication*). This highlights the importance of using predictive models to allocate survey efforts when studying patchy species with specific habitat preferences across a large range, an important issue when dealing with the budgetary, staffing, and timeline restrictions with which many field researchers are faced. Nevertheless, the model that was used to stratify field sites predicted the presence of *A. palmeri* at many sites in which the species was not detected. The low specificity incurred with each presence threshold method indicates a limited ability for the SDM to discriminate between suitable and un-suitable sites. Within the model selection process, reducing the number of input variables may have led to an overestimation of niche breadth, resulting in high sensitivity and low specificity. Additionally, the higher accuracy in the eastern range of *A. palmeri* indicates that more recent and precise presence records may help improve model performance, as it is in this region that more recent presence records were utilized.

While evaluation metrics are subject to a trade-off between errors of omission and commission, the management objective of the study ought to be considered when choosing a threshold method. Commission errors, reflected in low specificity, may be more acceptable than omission errors when generating distribution models to establish conservation guidelines (Boykin et al., 2007). Furthermore, the absence of *A. palmeri* at a given site does not necessarily mean the site is unsuitable habitat for *A. palmeri*. Rather, the limited dispersal capabilities of this species may have prevented colonization of these sites, or colonization may be limited by external circumstances such as habitat disturbance, woody encroachment, or invasive grass encroachment (*personal observation*), or even by shifting climatic conditions that were not reflected in the input variables used to generate the SDM; current layers derived from WorldClim only represent climatic norms between 1960 and 1990 (Hijmans et al., 2005). This study indicates that SDMs can serve as an important biogeographical tool to predict plant species ranges, while informing more detailed field studies to obtain finer scale habitat variables that influence species presence or absence within these ranges.

The most important variable in the SDM, precipitation during the warmest quarter, likely influences *A. palmeri* survival at multiple life stages. The warmest quarter of the year is likely when reproductive individuals flower, fruit, and disperse seed, with germination dependent on moist soil conditions promoted by summer monsoons. Additionally, young *Agave* spp. are more prone to desiccation due to limited water storage capacity, and are thus highly sensitive to moisture conditions (Nobel, 1988). While older plants may have an enhanced buffer to drought due to water storage in succulent leaves, new patches will not be colonized if conditions are not suitable for germination and juvenile recruitment. This should be of concern in the southwestern United States where conditions are expected to become hotter and drier (Seager et al., 2007), especially since *A. palmeri*, unlike most other *Agave* spp., does not reproduce vegetatively (Gentry, 1982). The long life cycle of *A. palmeri* makes this species especially vulnerable to changing climatic regimes since this limits the rate at which a population of *A. palmeri* can adapt to changing conditions. While genetic outcrossing by bats that travel long distances between foraging grounds may increase the resilience of *Agave* spp. to climate change (Fleming, 2009), patches of *Agave* spp. must have a high enough density of inflorescences to warrant pollinator visitation in order for such outcrossing to occur (Essenberg, 2012).

Based on the results of this study, we recommend several areas of further research. First, this model of *A. palmeri* distribution ought to be updated as more recent and higher resolution climatic variables become available, and more precise presence records of *A. palmeri* ought to be utilized. The standard methods employed in this study are easily repeatable and can be continually integrated with updated data. Also, GIS data for the Mexican states of Chihuahua and Sonora would allow the influence of an artificial boundary on the US–Mexico border to be assessed, while also helping to identify potential foraging grounds for nectarivorous bats in northern Mexico, an area that is largely understudied. We also recommend following these same methods for *Agave* spp. with the abilities to reproduce from bulbils, such as *A. lechuguilla, A. schottii,* or *A. parryi*, to see if reproductive strategies influence SDM accuracy. This would help indicate if the reproductive strategy of *A. palmeri* does in fact restrict niche breadth from that which is predicted in SDMs. Lastly, potential range shifts under various climate scenarios ought to be modeled to inform assisted migration plans for *A. palmeri*, as it may exhibit limited dispersal capabilities and a limited ability to effectively adapt to changing climates based on its limited dispersal and long life span. Future studies would be enhanced by collaboration between land managers, land owners, and researchers. Information generated from this study and future studies will be key in helping develop effective conservation plans for nectarivorous bats in the region.

5. Acknowledgements

Funding for this project came from T&E Inc., New Mexico Native Plant Society Otero Chapter, New Mexico Association of Conservation Districts, and the Department of Fish, Wildlife, and Conservation Ecology at New Mexico State University. This project was also made possible by a career development grant from the American Association of University Women. We would also like to thank Dr. Jennifer Frey for guidance with modeling methods, and Dr. Amy Ganguli and Dr. Patrick Alexander for project guidance and support. Lastly, we would like to thank our field assistant, Chelsey Trejo, for assisting with transects in all conditions, and the Butler Family for hosting us at their ranch in the San Rafael Valley while conducting field surveys.

CHAPTER 3.

CONCLUSION

This study is part of a larger project assessing habitat suitability for nectarivorous bats throughout the southwestern United States. By generating this species distribution model for *Agave palmeri*, the groundwork for further study has been established. While this model informed the sampling methodology for accuracy assessment in this study, the same sampling methodology was also followed to obtain more detailed information on *A. palmeri* populations and individuals. As a dual master's student in Applied Geography and Fish, Wildlife, and Conservation Ecology, I conducted a two-part project in which methods complimented one another. While this project in Applied Geography lays the groundwork for the study of *A. palmeri*, my Fish, Wildlife, and Conservation Ecology project builds upon this project in several ways.

In a follow up study, I investigate the relationship between the relative occurrence rate in the *A. palmeri* SDM and *A. palmeri* density on the ground, rather than presence or absence, to see if SDMs can help predict habitat quality for pollinators by representing resource density. I also investigate the influence of climatic conditions on the size class distribution of *A. palmeri*, using size class as a surrogate indicator of population trends. If low juvenile recruitment in *A. palmeri* patches is a major reason why potentially suitable regions are uninhabited by *A. palmeri*, exploring the climatic and land use variables behind this may help further inform decisions regarding *A. palmeri* management and restoration.

While conducting field work, several anecdotal observations were made regarding *A. palmeri* distribution. Many of the densest patches of *A. palmeri* observed in the field seemed to be in areas which we could not survey because they fell on private lands. It is possible that private land owners may be managing their property differently than federal land management agencies, and this warrants further investigation as well as collaboration among land owners and land managers. Within the area of study, *A. palmeri* patches on private lands were observed to occur on open hills, between the more rugged terrain in which *A. palmeri* occur on federal lands. These intermittent habitats may be critical in maintaining dispersal corridors between xeric mountain ranges for *A. palmeri*, as well as in maintaining nectar corridors for bats.

Secondly, there appeared to be a negative association between adult *A. palmeri* and forest cover, and a positive association between juvenile *A. palmeri* and forest cover. This will be further investigated in the follow up study, as it may indicate stages of ecological succession at which *A. palmeri* colonizes new patches. While *A. palmeri* may require nurse plants to germinate and establish juveniles, as many desert succulent plants do, there may come a point when competition for sunlight may inhibit growth and populations may not thrive unless there is a disturbance to the forest canopy. This represents one of the many possible reasons that *A. palmeri* were expected to occur in many sites in which they did not. *Agave palmeri* may also have negative associations with particular plant species, and positive associations with others, which will be assessed in a future study using an external dataset.

Thirdly, when looking at reproductive *A. palmeri*, herbivory rates appeared to be quite high. Native ungulates seemed to be the main culprit, as two hoof marks were often identified on the stalk below the point at which panicles were eaten. Water sources provided by wildlife managers may attract herbivores to patches of *A. palmeri* that neighbor these features, thus increasing herbivory risk.

As an overall conclusion, this study highlights several major findings regarding species distribution modeling for *A. palmeri*. Amongst the most notable is the extreme variation in predicted species ranges under various presence threshold methods. These differences are especially important to note when predicted ranges are used to inform management, or to estimate range shifts under climate change scenarios. It is unclear whether areas in which presence was predicted yet no *A. palmeri* occurred are actually unsuitable or if external circumstances prevented *A. palmeri* from occurring in those sites.

If sites where conditions are determined suitable for *A. palmeri* yet *A. palmeri* is not present at those sites, these may be targets for assisted migration to restore populations and enhance resource availability for nectarivorous bats. I recommend intersecting these regions with regions which are also within suitable habitat for nectarivorous bats to prioritize restoration sites for *A. palmeri*. Bat habitat models generated for my Fish, Wildlife, and Conservation Ecology project will help identify these sites. Given the potential susceptibility of *A. palmeri* to changing climatic conditions, I recommend targeting individuals based on their genetic diversity when attempting to restore populations from a limited number of individual plants. This ought to be investigated in a follow up study, as higher heterozygosity in *A. palmeri* will help increase population resilience to climate change.

REFERENCES

Allouche, O., Tsoar, A., and Kadmon, R. (2006). Assessing the accuracy of species distribution models: prevalence, Kappa and the true skill statistic (TSS). *Journal of Applied Ecology.* 43(6): 1223-1232.

Anderson, D. R. (2008). *Model based inferences in the life sciences: a primer on evidence*. Springer; New York, New York.

Anderson, R. P., and Gonzalez, I. Jr. (2011). Species-specific tuning increases robustness to sampling bias in models of species distributions: An implementation with Maxent. *Ecological Modelling*. 222: 2796-2811.

Arita, H. T., and Humphrey, S. R. (1988). Revisión taxonómica de los murciélagos magueyeros del género Leptonycteris (Chiroptera: Phyllostomidae). *Acta Zoologica Mexicana Nueva*. 29: 1-60.

Bellamy, C., Scott, C., and Altringham, J. (2013). Multiscale, presence-only habitat suitability models: fine-resolution maps for eight bat species. *Journal of Applied Ecology*. 50: 892-901

Boria, R. A., Olson, L. E., Goodman, S. M., Anderson, R. p. (2014). Spatial filtering to reduce sampling bias can improve the performance of ecological niche models. *Ecological Modelling.* 275: 73-77.

Boykin, K. G., B. C. Thompson, R. A. Deitner, D. Schrupp, D. Bradford, L. O'Brien, C. Drost, S. Propeck-Gray, W. Rieth, K. Thomas, W. Kepner, J. Lowry, C. Cross, B. Jones, T. Hamer, C. Mettenbrink, K.J. Oakes, J. Prior-Magee, K. Schulz, J. J. Wynne, C. King, J. Puttere, S. Schrader, and Z. Schwenke. 2007. Predicted animal habitat distributions and species richness. Chapter 3 in J.S. Prior-Magee, et al., eds. Southwest Regional Gap Analysis Final Report. U.S. Geological Survey, Gap Analysis Program, Moscow, ID.

Buja, K., and Menza, C. (2013). Sampling design tool for ArcGIS- Instruction Manual for ESRI ArcGIS 10.0 service pack or higher. *NOAA*.

Burnham, K. P. and Andersen, D. R. (2002). *Model selection and multimodal inference: a practical information-theoretic approach,* Second Edition. Springer-Verlag; New York, New York.

Cajas-Castillo, J. O., Kraker-Castañeda, C., López-Gutiérrez, J., Pérez-Consuerga, S. G., Grajeda-Godínez, A. L. (2015). *Choeronycteris mexicana* in Guatemala: temporal occurrence, feeding habits and reproductive activity. *Revista Mexicana de Biodiversidad.* 86(3): 835-838.

Elith, J., Phillips, S. J., Hastie, T., Dudík, Chee, Y. E., and Tates, C. J. (2011). A statistical explanation of Maxent for ecologists. *Diversity and Distributions*. 17: 43-57.

England, A. E. (2012). Pollination ecology of *Agave palmeri* in New Mexico, and landscape use of *Leptonycteris nivalis* in relation to Agaves. Biology ETDs. Paper 31.

Fleming, T. H., Geiselman, C., and Kress, W. J. (2009). The evolution of bat pollination: a phylogenetic perspective. *Annals of Botany* (104): 1017-1043.

Fleming, T. H., Nuñez, R. A., and Stenberg, L. S. L. (1993). Seasonal changes in the diets of migrant and non-migrant nectivorous bats as revealed by carbon stable isotope analysis. *Oecologia* (94): 72-75

Freeman, E. A., and Moisen, G. G. (2008). A comparison of the performance of threshold criteria for binary classification in terms of predicted prevalence and kappa. *Ecological Modelling*. 217: 48-58.

Frey, J. K., Lewis, J. C., Guy, R. K., and Stuart, J. N. (2013). Use of anecdotal occurrence data in species distribution models: an example based on the white-nosed coati (Nasua narica) in the American Southwest. *Animals* (3): 327-348.

Gentry, H. S. (1982). *Agaves of continental North America*, 670 pp. University of Arizona Press, Tucson.

Godínez-Alvarez, H., and Valiente-Banuet, A. (2000). Fruit-feeding behavior of the bats Leptonycteris curasoae and Choeronycteris mexicana in flight cage experiments: consequences for dispersal of columnar cactus seeds. *Biotropica* (32): 552-556.

Gorresen, M., Willig, M. R., and Strauss, R. E. (2005). Multivariate analysis of scale-dependent associations between bats and landscape structure. *Ecological Applications*. 15(6): 2126-2136.

Hayes, M. A., Cryan, P. M., and Wunder, M. B. (2015). Seasonally-dynamic presence-only species distribution models for a cryptic migratory bat impacted by wind energy development. *PLoS ONE*. 10(7): e0132599. doi:10.1371/ journal.pone.0132599

Hijmans, R.J., S.E. Cameron, J.L. Parra, P.G. Jones and A. Jarvis, 2005. Very high resolution interpolated climate surfaces for global land areas. *International Journal of Climatology* (25): 1965-1978.

Hijmans, R. J. (2015). Introduction to the 'raster' package (version 2.4-20). https://cran.r-project.org/web/packages/raster/vignettes/Raster.pdf. Accessed 11/2/2015.

Horner, M. A., Fleming, T. H., and Sahley, C. T. (1998). Foraging behavior and energetics of a nectar-feeding bat, Leptonycteris curasoae (Chiroptera: Phyllostomidae). *Journal of Zoology*, London (244): 575-586.

Howell, D.J. and Roth B.S. (1981). Sexual reproduction in agaves: the benefits of bats; the cost of semelparous advertising. *Ecology* (62): 1–7.

Hoyt, R. A., J. S. Altenbach, and D. J. Hafner. 1994. Observations on long-nosed bats (*Leptonyceris*) in New Mexico. *Southwestern Naturalist.* (39): 175-179.

Johnson, J. B., and Omland, K. S. (2004). Model selection in ecology and evolution. *Trends in Ecology and Evolution*. 19(2): 101-108.

Liu, C., Berry, P. M., Dawson, T. P., Pearson, R. G. (2005). Selecting thresholds of occurrence in the prediction of species distributions. *Ecography*. 28(3): 385-393.

Liu. C., White, M., and Newell, G. (2011). Measuring and comparing the accuracy of species distribution models with presence-absence data. *Ecography*. 34(2): 232-243.

Liu, C. Newell, G., White, M. (2016). On the selection of thresholds for predicting species occurrence with presence-only data. *Ecology and Evolution*. 6(1): 337-348.

MacKenzie, D.I., Nichols, J.D., Royle, J.A., Pollock, K.H., Bailey, L.L. & Hines J.E. (2006). *Occupancy Estimation and Modeling: Inferring Patterns and Dynamics of Species Occurrence*. Academic Press, New York.

MacKenzie, D. I., Nichols, J. D., Lachman, G. B., Droege, S., Royle, A., and Langtimm, C. A. (2002). Estimating occupancy rates when detection probabilities are less than one. *Ecology*. 83(8): 2248-2255.

Merow, C., Smith, M. J., Silander, J. A., Jr. (2013). A practical guide to MaxEnt for modeling species' distributions: what it does, and why inputs and settings matter. *Ecography.* 36: 1058-1069.

Nenzén, H. K. and Araújo, M. B. (2011). Choice of threshold alters projections of species range shifts under climate change. *Ecological Modeling*. 222: 3346-3354.

Nichols, J. D., Bailey, L. L., O'Connell, A. F. Jr., Talancy, N. W., Campbell Grant, E. H., Gilbert, A. T., Annand, E. M., Husband, T. P., and Hines, J. E. (2008). Multi-scale occupancy estimation and modeling using multiple detection methods. *Journal of Applied Ecology*;. 45: 1321-1329.

Norris, D. (2014). Model thresholds are more important than presence location type: Understanding the distribution of lowland tapir (*Tapirus terrestris*) in a continuous Atlantic forest of southeast Brazil. *Tropical Conservation Science*. 7(3): 529-547.

Olson, G. S., Anthony, R. G., Forsman, E. D., Ackers, S. H., Loschl, P. J., Reid, J. A., Dugger K. M., Glenn, E. M., and Ripple, W. J. (2005). Modeling of site occupancy dynamics for northern spotted owls, which emphasis on the effects of barred owls. *Journal of Wildlife Management*. 69: 918-932.

Phillips, S. J., Anderson, R. P., Schapire, R. E. 2006. Maximum entropy modeling of species geographic distributions. *Ecological Modelling.* 190: 231-259.

Phillips, S. J., Dudik, M., Elith, J., Graham, C. H., Lehmann, A., Leathwick, J., and Ferrier, S. (2009). Sample selection bias and presence-only distribution models: implications for background and pseudo-absence data. *Ecological Applications*; 19(1): 181-197.

Ober, H. K., and Steidl, R. J. (2004). Foraging rates of *Leptonycteris curasoae* vary with characteristics of Agave palmeri. *Southwestern Naturalist.* 49*(*1), 68-74.

Rainho, A. and Palmerin, J. M. 2011. The importance of distance to resources in the spatial modeling of bat foraging habitat. PloS One 6: e19227.

Razgour, O., Hammer, J., and Jones, G. 2011. Using multi-scale modeling to predict habitat suitability for species of conservation concern: The grey long-eared bat as a case study. *Biological Conservation*; 144: 2922-2930.

Rebelo, H. and Jones, G. (2010). Ground validation of presence-only modeling with rare species: a case study on barbastelles *Barbastella barbastellus* (Chriptera: Vespertillionidae). *Journal of Applied Ecology*. doi: 10.1111/j.1365-2664.2009.01765.x

Robinson, Q. H., Bustos, D., and Roemer, G. W. (2014). The application of occupancy modeling to evaluate intraguild predation in a model carnivore system. *Ecology*. 95(11): 3112-3123.

Rocha, M., Good-Avíla, S. V., Molina-Freaner, F., Arita, H. T., Castillo, A., García-Mendosa, A., Silva-Montellana, A., Gaut, B. S., Souza, V., and Eguiarte. L. E. (2006). Pollination biology and adaptive radiation of Agavaceae, with special emphasis on the genus *Agave*. *Aliso* (22): 329-344.

Rojas-Martínez, A., Godínez-Alvarez, H., Valiente-Banuet, A., Arizmendi, A. d. C., Acevedo. O. S. (2012). Fruigvory diet of the lesser long-nosed bat (*Leptonycterus yerbabuenae*), in the Tehuacán Valley of Central Mexico. *Edición especial los mam*íferos de Oaxaca. 3(3): 371-380.

Rojas-Martínez, A., Valiente-Banuet, A., Arizmendi, M., Alcántara-Eguren, A., Arita, H. (1999). Seasonal distribution of the long-nosed bat (*Leptonycteris curasoae*) in North America: does a generalized migration pattern really exist? *Journal of Biogeography*. 26: 1065-1077.

Scott, P. E. (2004). Timing of *Agave palmeri* flowering and nectar-feeding bat visitation in the Peloncillos and Chiricahua Mountains. *The Southwestern Naturalist*. 49(4): 425-434.

Searcy, C. A. and Shaffer, B. (2014). Field validation supports novel niche modeling strategies in a cryptic endangered amphibian. *Ecography;* 37: 983-992.

Slauson, L. A. (1999). Pollination biology of two chiropterophilous agaves in Arizona. *American Journal of Botany*. 87(6): 825-836.

Soil Survey Staff, Natural Resources Conservation Service, United States Department of Agriculture. Soil Survey Geographic (SSURGO) Database. Available online at https://sdmdataaccess.sc.egov.usda.gov. Accessed [5/1/2016].

Stoner, K. E., O.-Salazer, K. A., R.-Fernández, R.C., and Quesada, M. (2003). Population dynamics, reproduction, and diet of the lesser long-nosed bat (*Leptonycteris curasoae*) in Jalisco, Mexico: implications for conservation. *Biodiversity and Conservation* (12): 357-373.

U.S. Fish and Wildlife Service. 1994. Mexican Long-Nosed Bat (*Leptonycteris nivalis*) Recovery Plan. U.S. Fish and Wildlife Service, Albuquerque, New Mexico. 91 pp.

U.S. Fish and Wildlife Service. 1995. Lesser Long-Nosed Bat Recovery Plan. U.S. Fish and Wildlife Service, Albuquerque, New Mexico. 45 pp.

USGS, Gap Analysis Program (GAP). May 2016. Protected Areas Database of the United States (PAD-US), version 1.4 Combined Feature Class.

USGS (2006), Shuttle Radar Topography Mission, 1 Arc Second scene, SRTM1N31W110V3; SRTM1N32W110V3; RTM1N31W109V3; SRTM1N32W109V3; SRTM1N31W108V3; SRTM1N32W108V3; SRTM1N33W110V3; SRTM1N33W109V3; SRTM1N32W112V3; SRTM1N33W112V3; SRTM1N33W111V3; SRTM1N33W113V3; SRTM1N31W113V3; SRTM1N32W113V3; SRTM1N31W112V3; SRTM1N31W111V3; SRTM1N32W111V3. Filled Finished, 2.0. Global Land Cover Facility, University of Maryland, College Park, Maryland, February 2000.

USGS National Gap Analysis Program. 2004. Provisional Digital Land Cover Map for the Southwestern United States. Version 1.0. RS/GIS Laboratory, College of Natural Resources, Utah State University.

USGS Open-File Report 2005a-1351 Preliminary integrated geologic map databases for the United States: Central states: Montana, Wyoming, Colorado, New

Mexico, North Dakota, South Dakota, Nebraska, Kansas, Oklahoma, Texas, Iowa, Missouri, Arkansas, and Louisiana. http://pubs.usgs.gov/of/2005/1351/

USGS Open-File Report 2005b-1305. Preliminary integrated geologic map databases for the United States - western states: California, Nevada, Arizona, Washington, Oregon, Idaho, and Utah. http://pubs.usgs.gov/of/2005/1305/

Van Proosdij, A.s.J., Sosef, M. S. M., and Wieri. J. J. (2015). Minimum required number of specimen records to develop accurate species distribution models. *Ecography*. (online before print). 27 pp.

Warren, D. L., Glor, R. E., Turello, M. (2008). Environmental niche equivalency versus conservativism: quantitative approaches to niche evolution. *Evolution*. 62(11): 2868-2883.

Warren, D. L., Glor, R., and Turelli, M. 2010. ENMTools: a toolbox for comparative studies of environmental niche models. *Ecography* 33: 607-611.

Warren, D. K., and Seifert, S. N. (2011). Ecological niche modeling in Maxent: the importance of model complexity and the performance of model selection criteria. *Ecological Applications.* 21(2): 335-342.

Warren, D. L., Wright, A. N., Seifert, S. N., Shaffer, H. B., 2014. Incorporating model complexity and spatial sampling bias into ecological niche models of climate change risks faced by 90 California vertebrate specie of concern. *Diversity and Distributions* 20: 334-343.

Wilkinson, G. S., and Fleming, T. H. (1996) Migration and evolution of lesser long-nosed bats *Leptonycteris curasoae*, inferred from mitochondrial DNA. *Molecular Ecology*. 5: 329-339.

Young, N., Evangelista, P., and Carter, L. (2011). A Maxent model v3.3.1 tutorial (ArcGIS v10). Colorado State University. http://ibis.colostate.edu/WebContent/WS/ColoradoView/TutorialsDownloads/Other_Tutorial1.pdf

APPENDIX

ENVIRONMENTAL LAYERS

All layers are shown in the format in which they were utilized in MaxEnt. These are unprojected ASCII layers in WGS 1984 datum used as environmental layers in the model selection process.

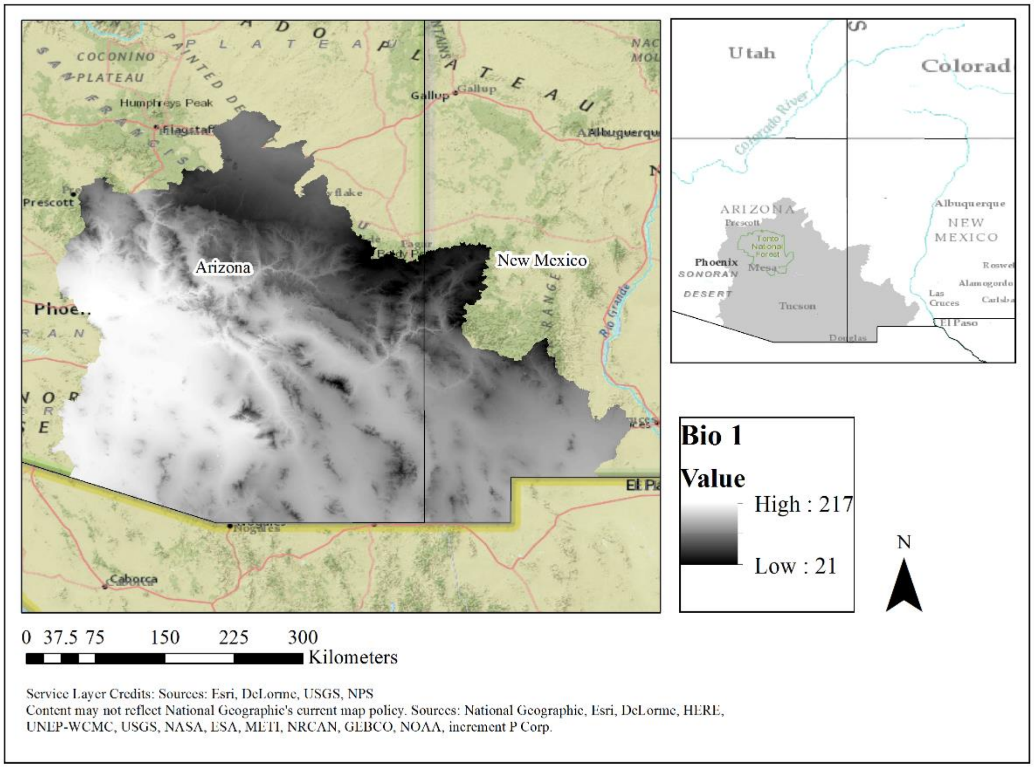

Service Layer Credits: Sources: Esri, DeLorme, USGS, NPS
Content may not reflect National Geographic's current map policy. Sources: National Geographic, Esri, DeLorme, HERE, UNEP-WCMC, USGS, NASA, ESA, METI, NRCAN, GEBCO, NOAA, increment P Corp.

Figure A. Bio 1, Annual Mean Temperature. Shown in Degrees Celsius times 10**. (**Hijmans et al., 2005)

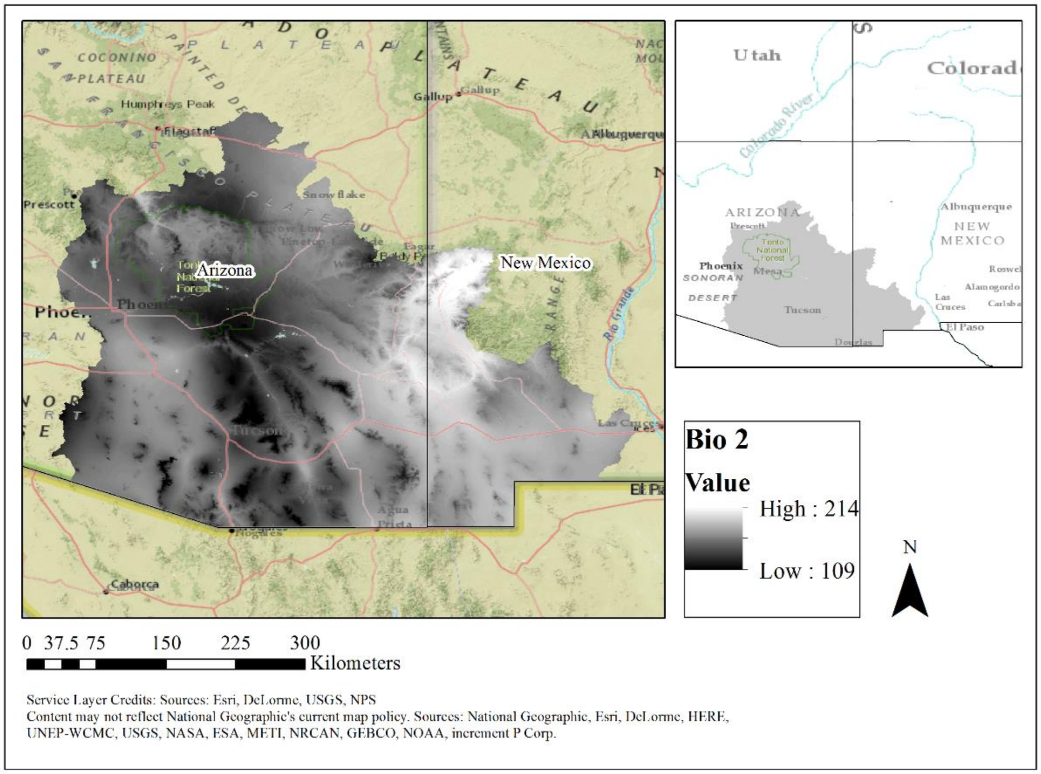

Service Layer Credits: Sources: Esri, DeLorme, USGS, NPS
Content may not reflect National Geographic's current map policy. Sources: National Geographic, Esri, DeLorme, HERE, UNEP-WCMC, USGS, NASA, ESA, METI, NRCAN, GEBCO, NOAA, increment P Corp.

Figure B. Bio 2. Mean Diurnal Range. (Mean of monthly difference between maximum temperature and minimum temperature). Shown in Degrees Celsius times 10 (Hijmans et al., 2005).

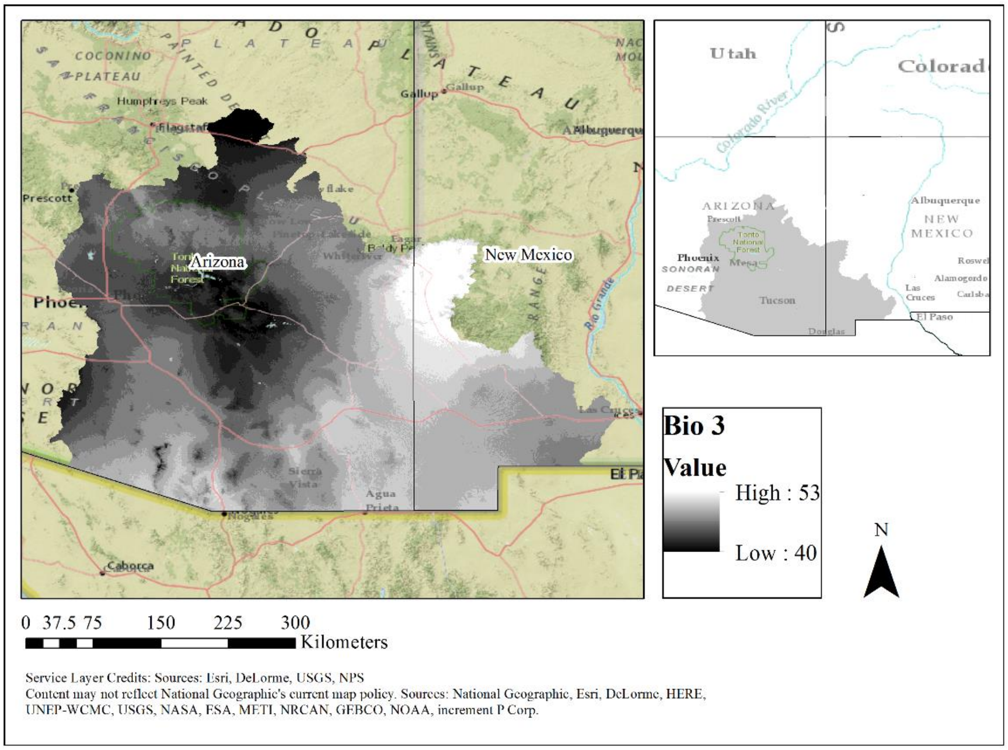

Figure C. Bio 3. Isothermality. Bio2 / Bio 7 * 100. (Mean monthly temperature / annual temperature range) * 100). (Hijmans et al., 2005).

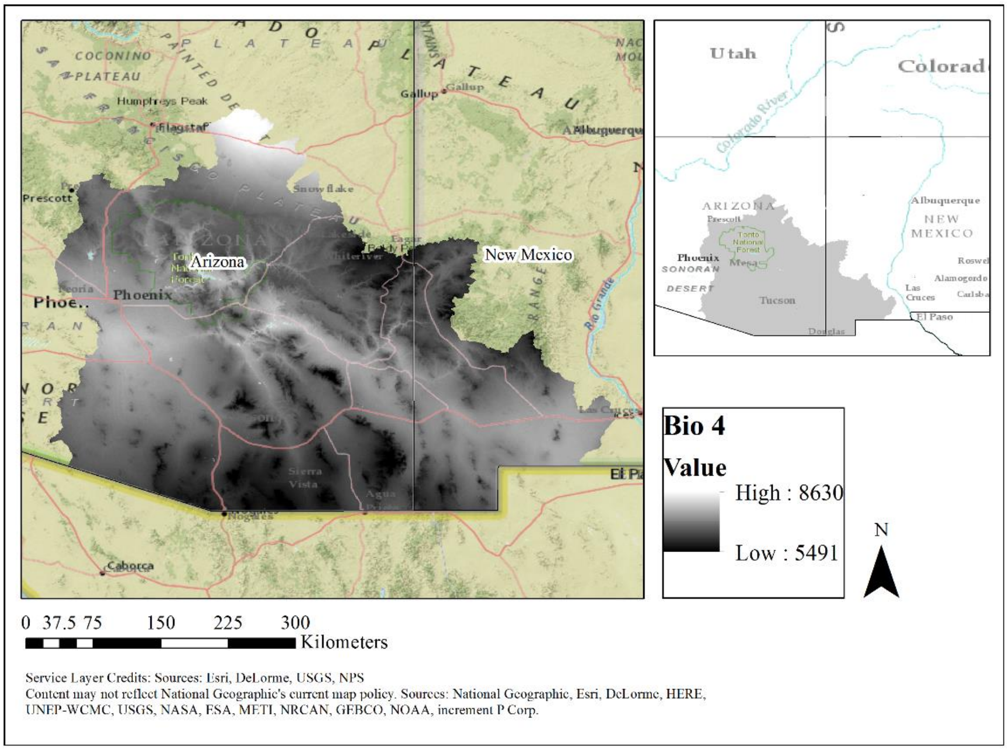

Service Layer Credits: Sources: Esri, DeLorme, USGS, NPS
Content may not reflect National Geographic's current map policy. Sources: National Geographic, Esri, DeLorme, HERE, UNEP-WCMC, USGS, NASA, ESA, METI, NRCAN, GEBCO, NOAA, increment P Corp.

Figure D. Bio 4. Temperature Seasonality (Standard deviation * 100). (Hijmans et al., 2005).

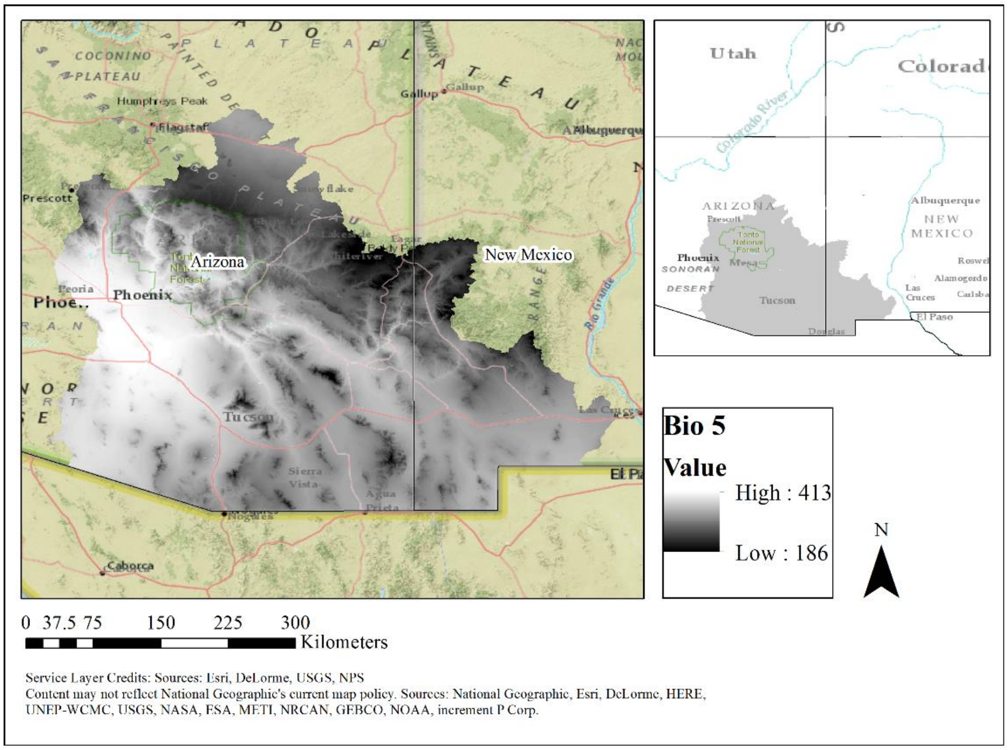

Service Layer Credits: Sources: Esri, DeLorme, USGS, NPS
Content may not reflect National Geographic's current map policy. Sources: National Geographic, Esri, DeLorme, HERE, UNEP-WCMC, USGS, NASA, ESA, METI, NRCAN, GEBCO, NOAA, increment P Corp.

Figure E. Bio 5. Maximum temperature of the warmest month. Shown in Degrees Celsius times 10. (Hijmans et al., 2005).

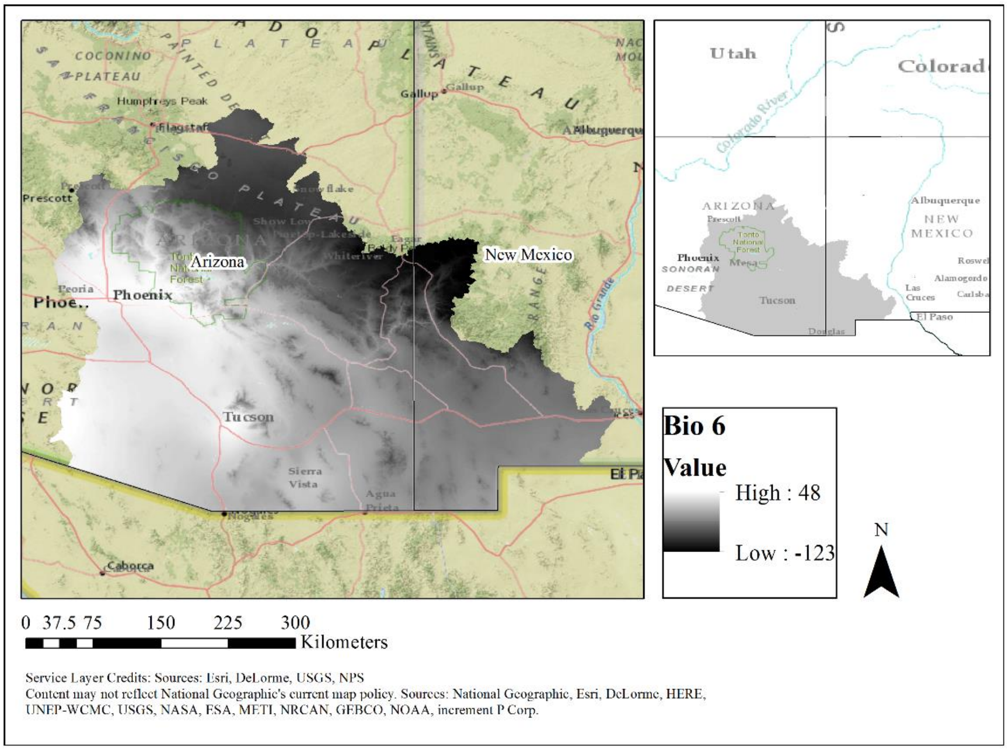

Service Layer Credits: Sources: Esri, DeLorme, USGS, NPS
Content may not reflect National Geographic's current map policy. Sources: National Geographic, Esri, DeLorme, HERE, UNEP-WCMC, USGS, NASA, ESA, METI, NRCAN, GEBCO, NOAA, increment P Corp.

Figure F. Bio 6. Minimum temperature of the coldest month. Shown in Degrees Celsius times 10. (Hijmans et al., 2005).

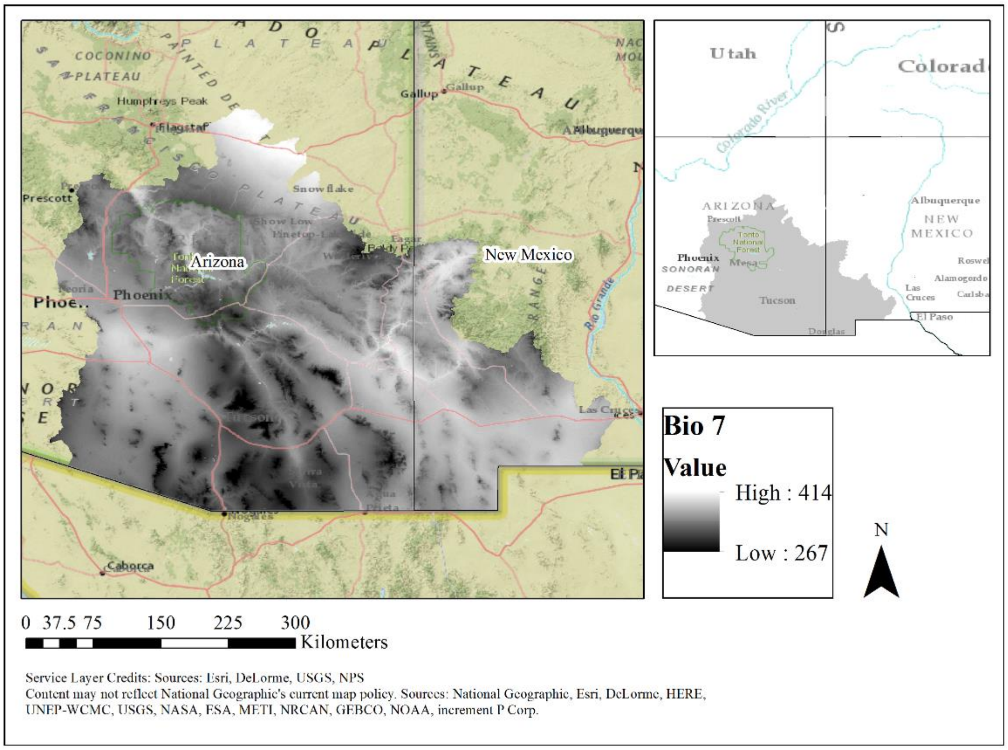

Service Layer Credits: Sources: Esri, DeLorme, USGS, NPS
Content may not reflect National Geographic's current map policy. Sources: National Geographic, Esri, DeLorme, HERE, UNEP-WCMC, USGS, NASA, ESA, METI, NRCAN, GEBCO, NOAA, increment P Corp.

Figure G. Bio 7. Temperature annual range (Bio 5 – Bio 6). Shown in Degrees Celsius times 10. (Hijmans et al., 2005).

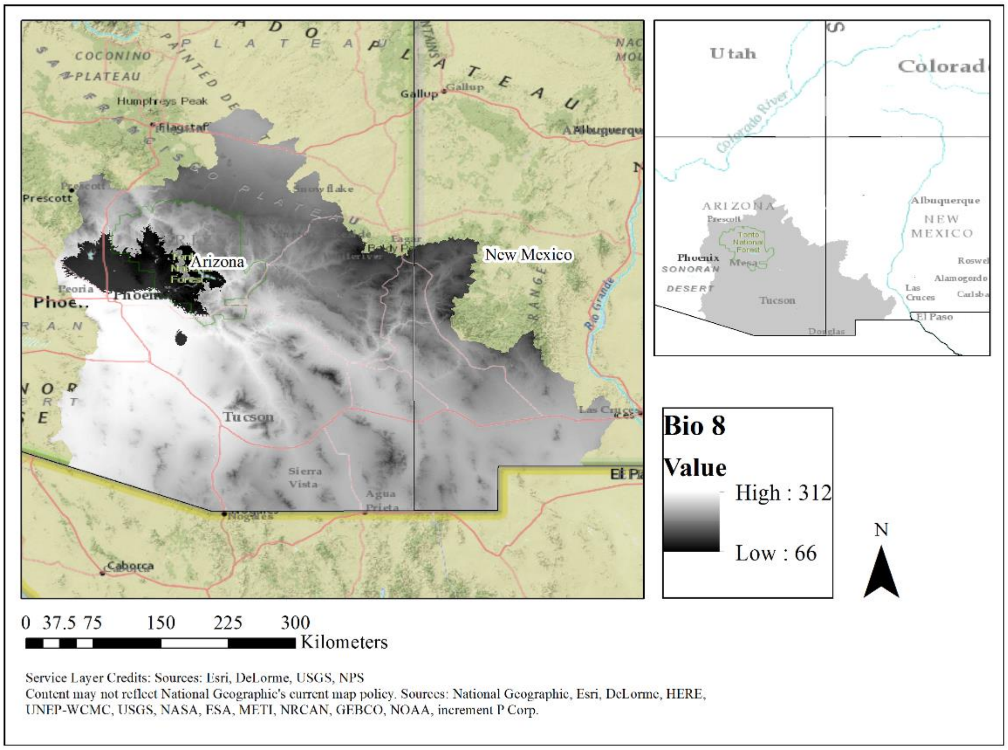

Service Layer Credits: Sources: Esri, DeLorme, USGS, NPS
Content may not reflect National Geographic's current map policy. Sources: National Geographic, Esri, DeLorme, HERE, UNEP-WCMC, USGS, NASA, ESA, METI, NRCAN, GEBCO, NOAA, increment P Corp.

Figure H. Bio 8. Mean temperature of the wettest quarter. Shown in Degrees Celsius times 10. (Hijmans et al., 2005). There appears to be an anomaly in the northwest corner of this layer, though it should not have influenced the model because Bio 8 had 0 % contribution to the final model.

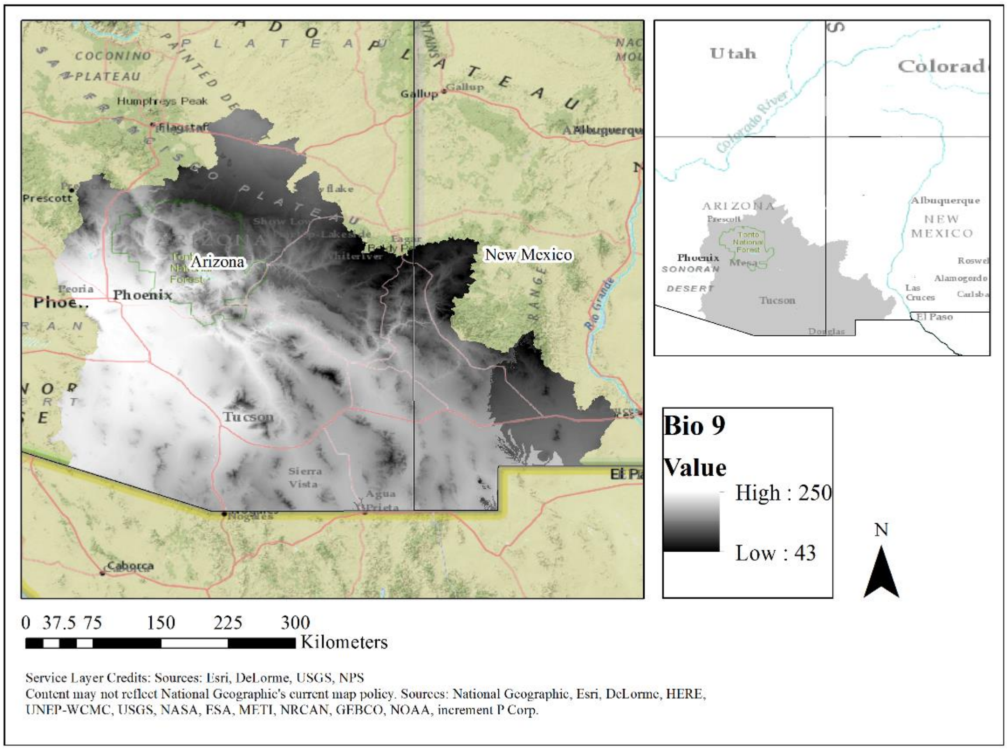

Service Layer Credits: Sources: Esri, DeLorme, USGS, NPS
Content may not reflect National Geographic's current map policy. Sources: National Geographic, Esri, DeLorme, HERE, UNEP-WCMC, USGS, NASA, ESA, METI, NRCAN, GEBCO, NOAA, increment P Corp.

Figure I. Bio 9. Mean temperature of the driest quarter. Shown in Degrees Celsius times 10. (Hijmans et al., 2005).

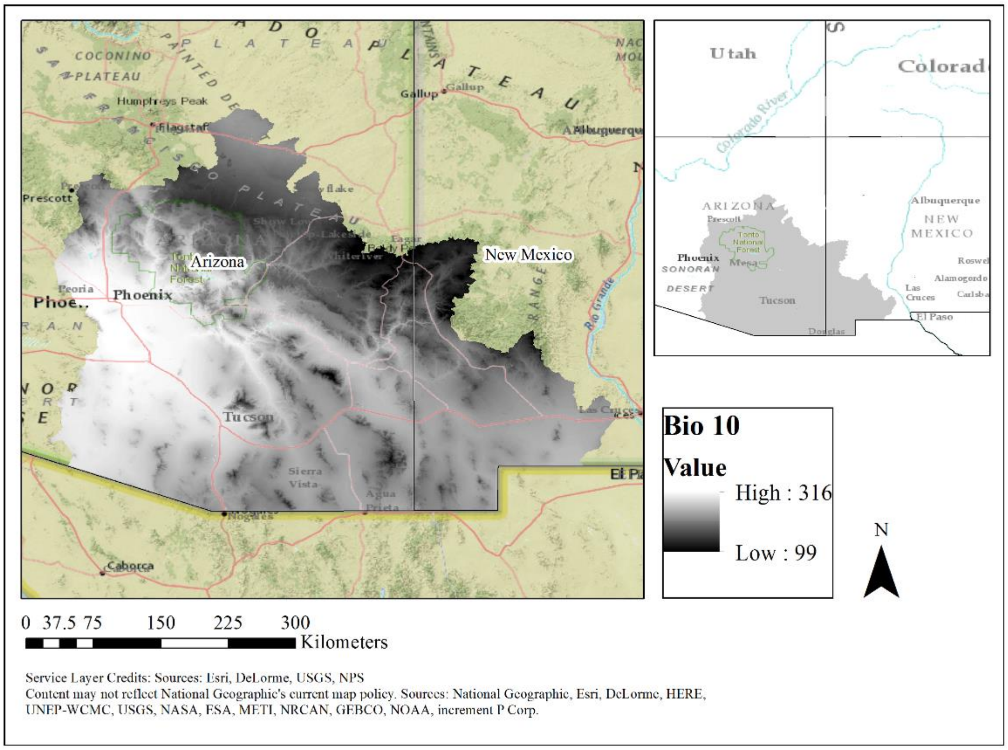

Service Layer Credits: Sources: Esri, DeLorme, USGS, NPS
Content may not reflect National Geographic's current map policy. Sources: National Geographic, Esri, DeLorme, HERE, UNEP-WCMC, USGS, NASA, ESA, METI, NRCAN, GEBCO, NOAA, increment P Corp.

Figure J. Bio 10. Mean temperature of the warmest quarter. Shown in Degrees Celsius times 10. (Hijmans et al., 2005).

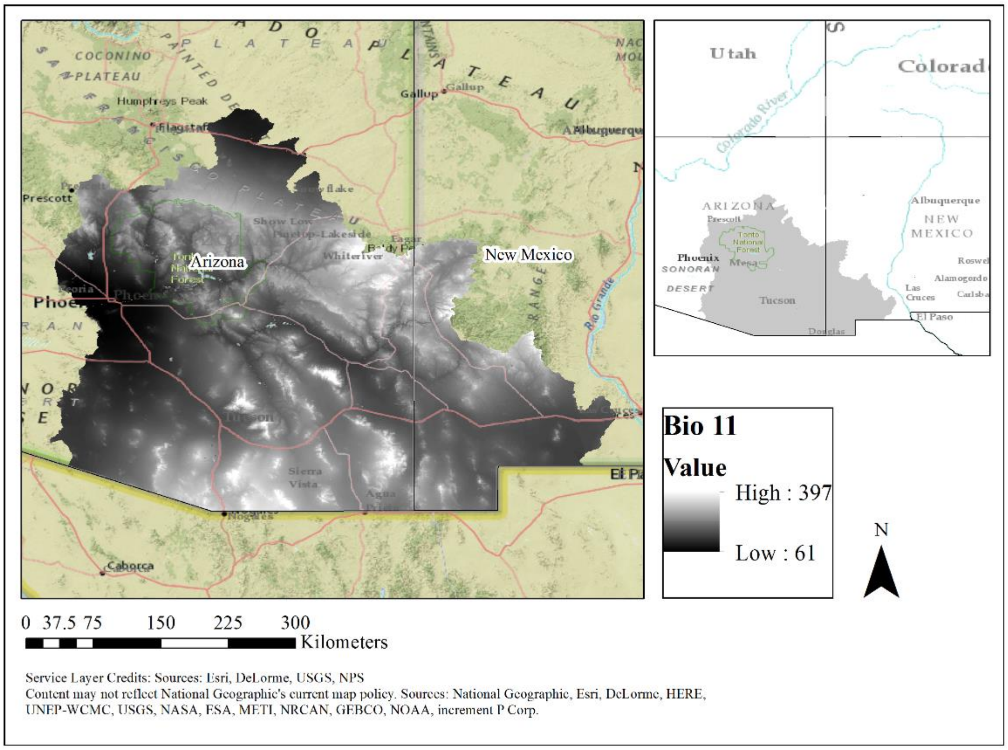

Figure K. Bio 11. Mean temperature of the coldest quarter. Shown in Degrees Celsius times 10. (Hijmans et al., 2005).

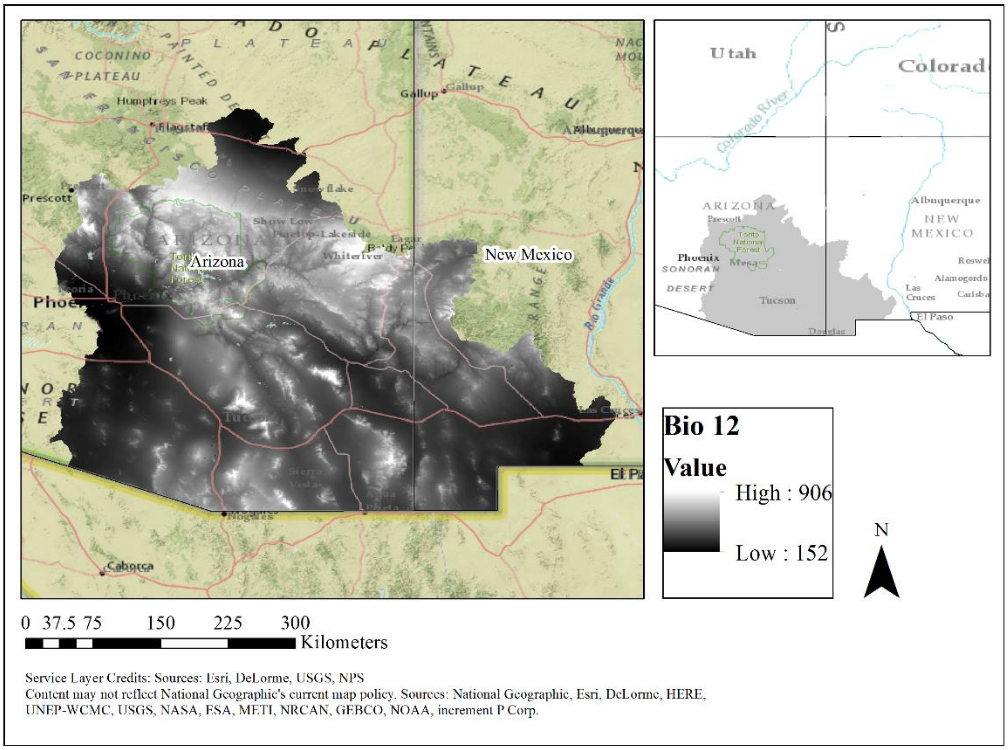

Service Layer Credits: Sources: Esri, DeLorme, USGS, NPS
Content may not reflect National Geographic's current map policy. Sources: National Geographic, Esri, DeLorme, HERE, UNEP-WCMC, USGS, NASA, ESA, METI, NRCAN, GEBCO, NOAA, increment P Corp.

Figure L. Bio 12. Annual precipitation (mm) (Hijmans et al., 2005).

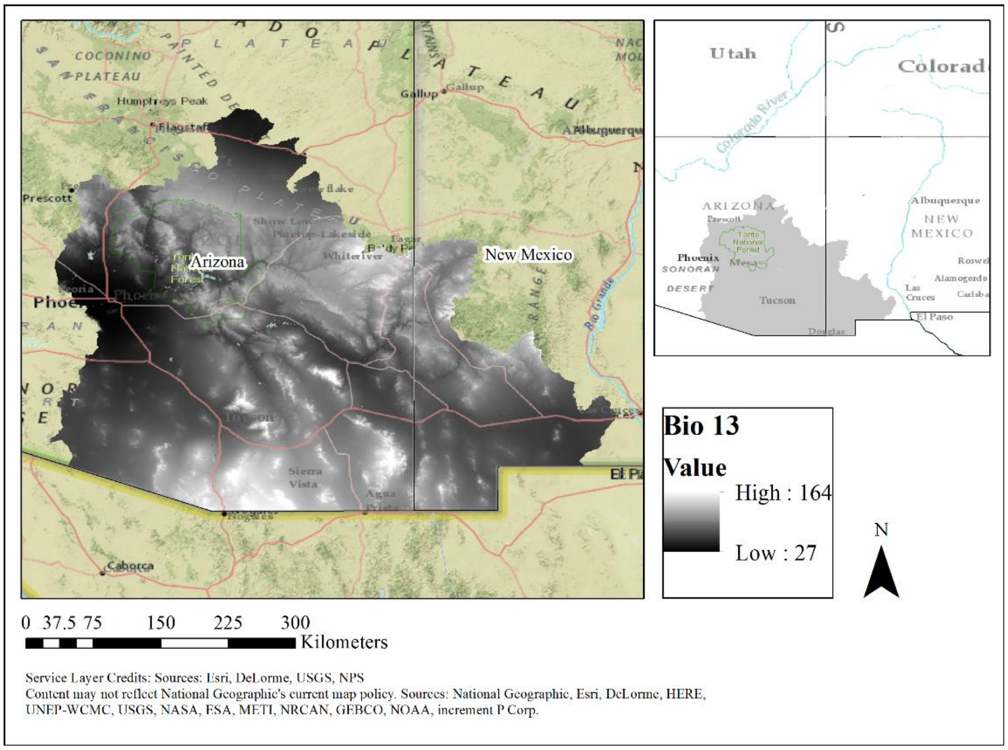

Figure M. Bio 13. Precipitation of the wettest month (mm). (Hijmans et al., 2005).

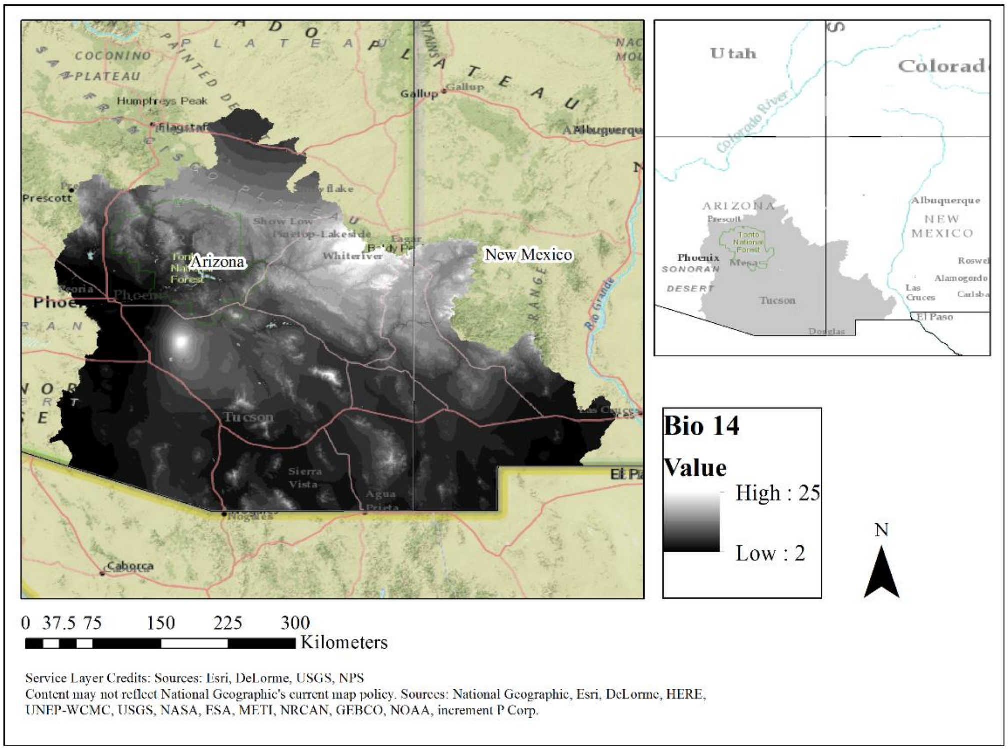

Service Layer Credits: Sources: Esri, DeLorme, USGS, NPS
Content may not reflect National Geographic's current map policy. Sources: National Geographic, Esri, DeLorme, HERE, UNEP-WCMC, USGS, NASA, ESA, METI, NRCAN, GEBCO, NOAA, increment P Corp.

Figure N. Bio 14. Precipitation of the driest month (mm). (Hijmans et al., 2005).

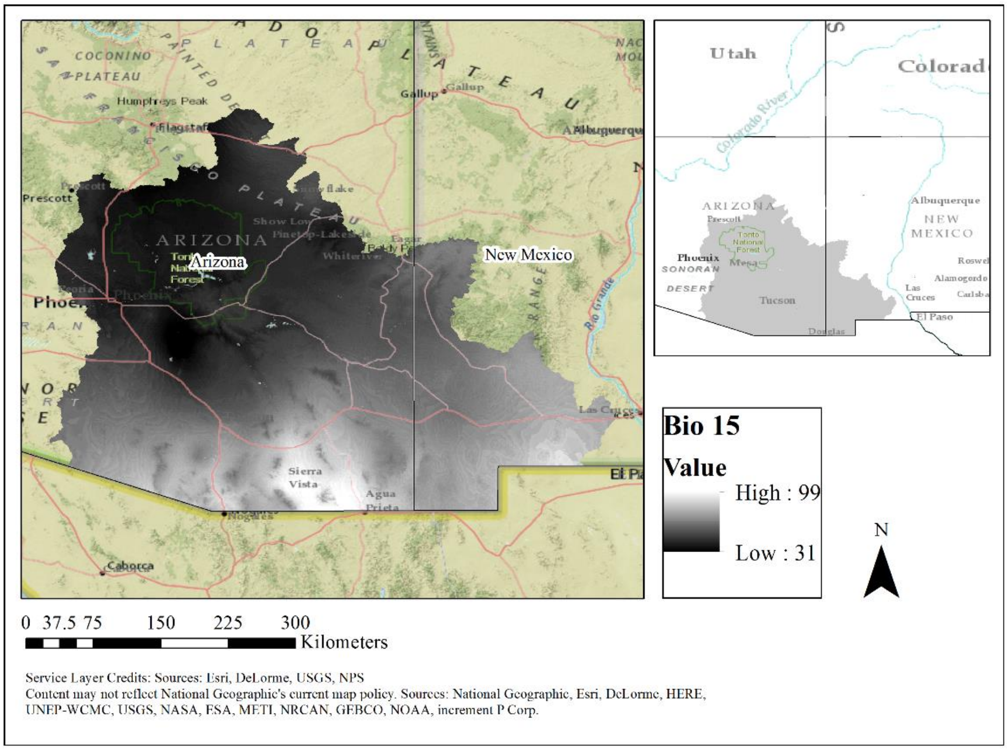

Service Layer Credits: Sources: Esri, DeLorme, USGS, NPS
Content may not reflect National Geographic's current map policy. Sources: National Geographic, Esri, DeLorme, HERE, UNEP-WCMC, USGS, NASA, ESA, METI, NRCAN, GEBCO, NOAA, increment P Corp.

Figure O. Bio 15. Precipitation seasonality (mm). (Coefficient of variation). (Hijmans et al., 2005).

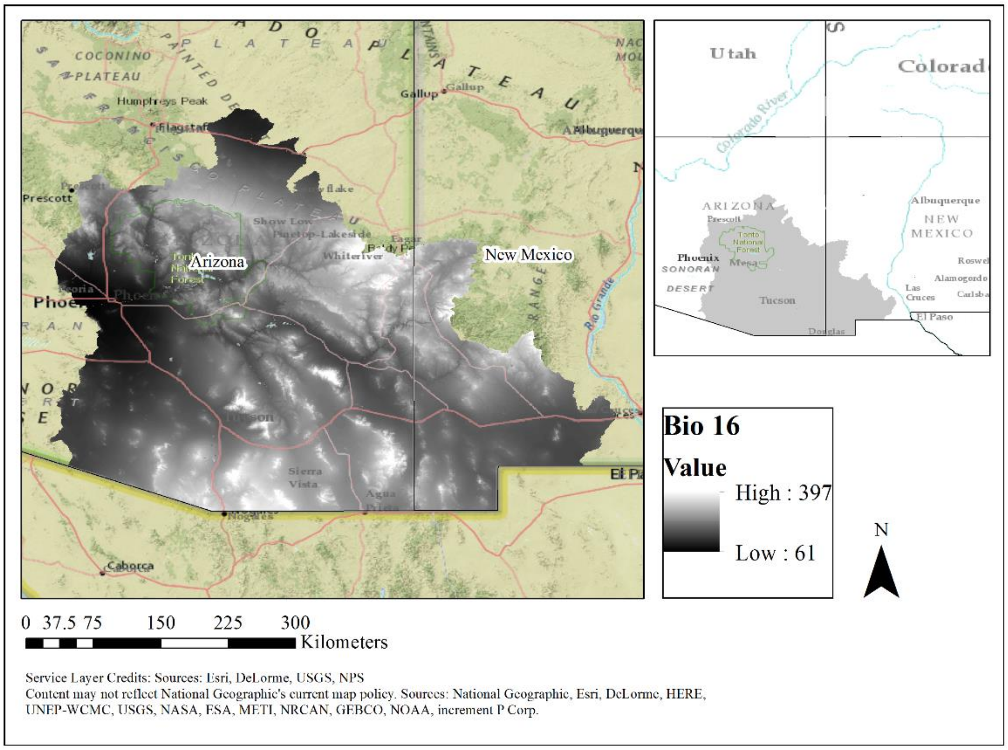

Figure P. Bio 16. Precipitation of the wettest quarter (mm). (Hijmans et al., 2005).

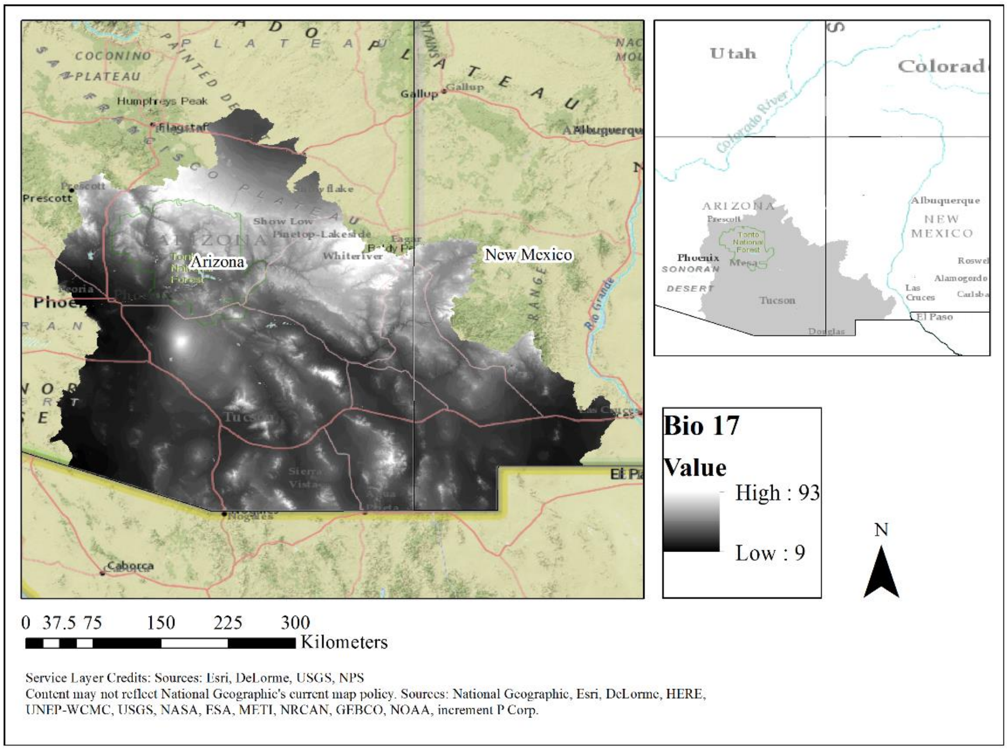

Service Layer Credits: Sources: Esri, DeLorme, USGS, NPS
Content may not reflect National Geographic's current map policy. Sources: National Geographic, Esri, DeLorme, HERE, UNEP-WCMC, USGS, NASA, ESA, METI, NRCAN, GEBCO, NOAA, increment P Corp.

Figure Q. Bio 17. Precipitation of the driest quarter (mm). (Hijmans et al., 2005).

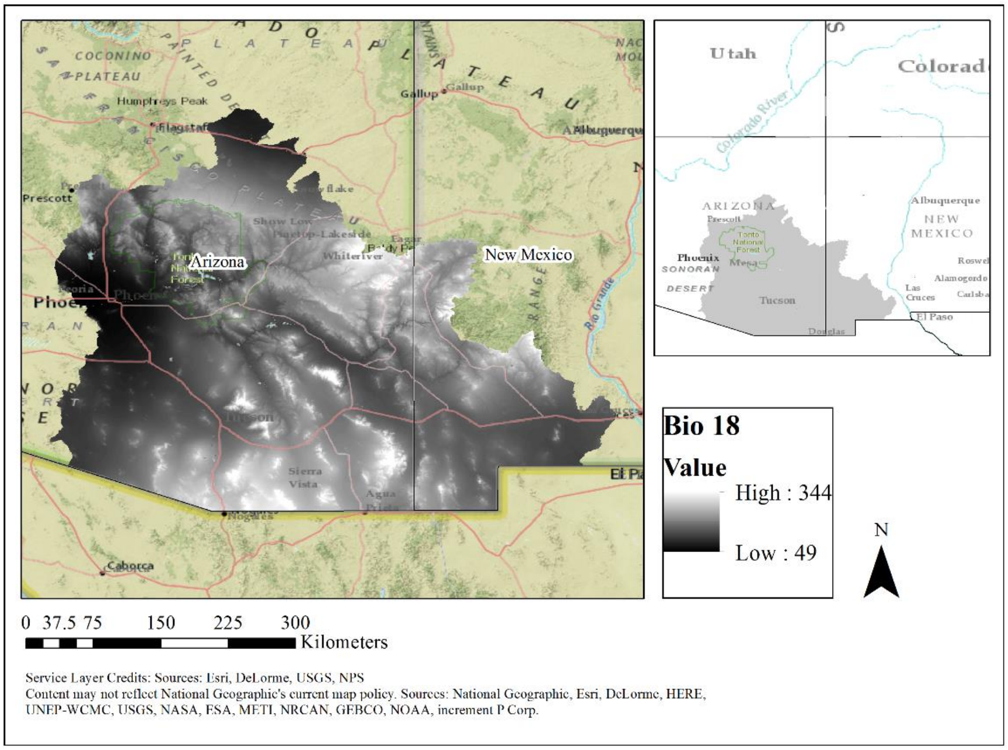

Service Layer Credits: Sources: Esri, DeLorme, USGS, NPS
Content may not reflect National Geographic's current map policy. Sources: National Geographic, Esri, DeLorme, HERE, UNEP-WCMC, USGS, NASA, ESA, METI, NRCAN, GEBCO, NOAA, increment P Corp.

Figure R. Bio 18. Precipitation of the warmest quarter (mm). (Hijmans et al., 2005).

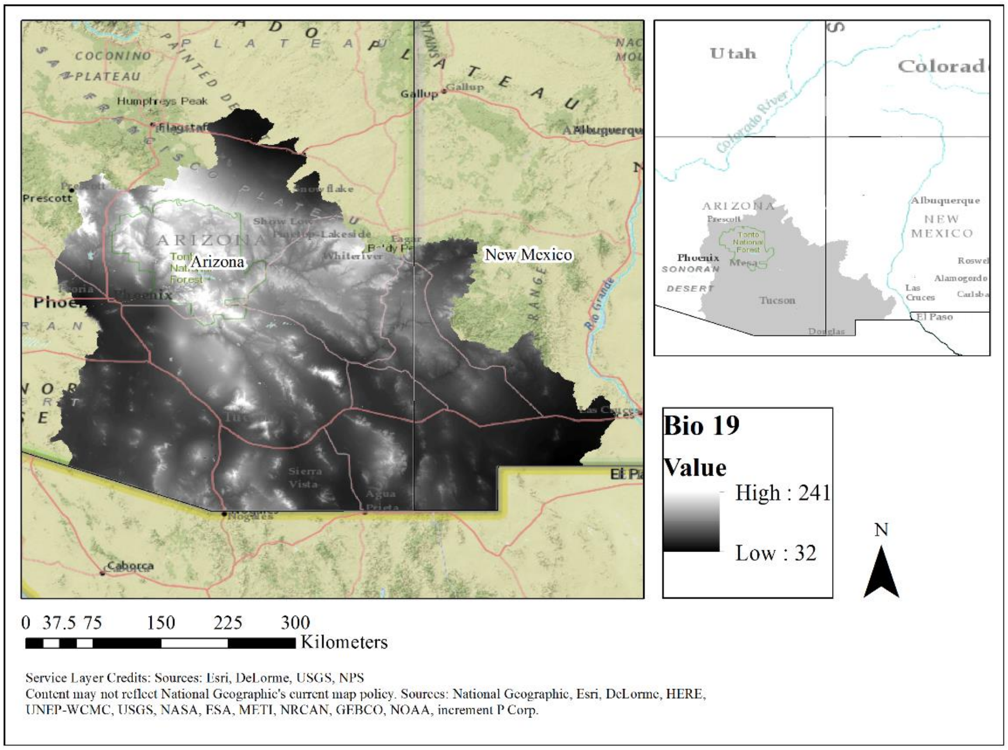

Service Layer Credits: Sources: Esri, DeLorme, USGS, NPS
Content may not reflect National Geographic's current map policy. Sources: National Geographic, Esri, DeLorme, HERE, UNEP-WCMC, USGS, NASA, ESA, METI, NRCAN, GEBCO, NOAA, increment P Corp.

Figure S. Bio 19. Precipitation of the coldest quarter (mm). (Hijmans et al., 2005).

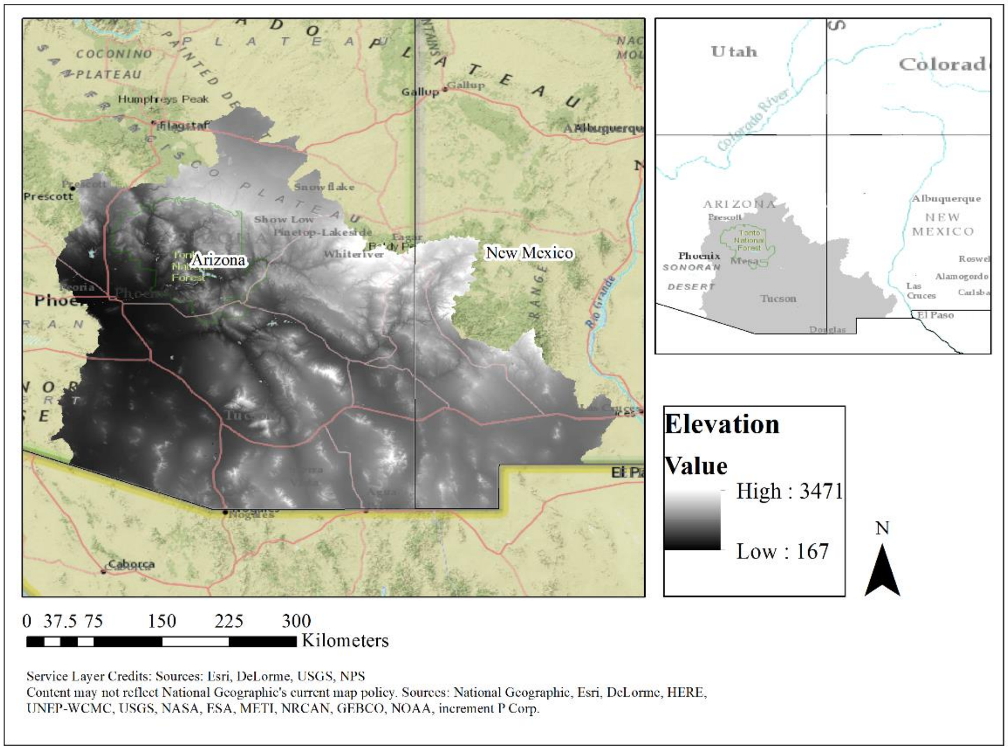

Service Layer Credits: Sources: Esri, DeLorme, USGS, NPS
Content may not reflect National Geographic's current map policy. Sources: National Geographic, Esri, DeLorme, HERE, UNEP-WCMC, USGS, NASA, ESA, METI, NRCAN, GEBCO, NOAA, increment P Corp.

Figure T. Elevation (m). Derived from SRTM (USGS, 2006).

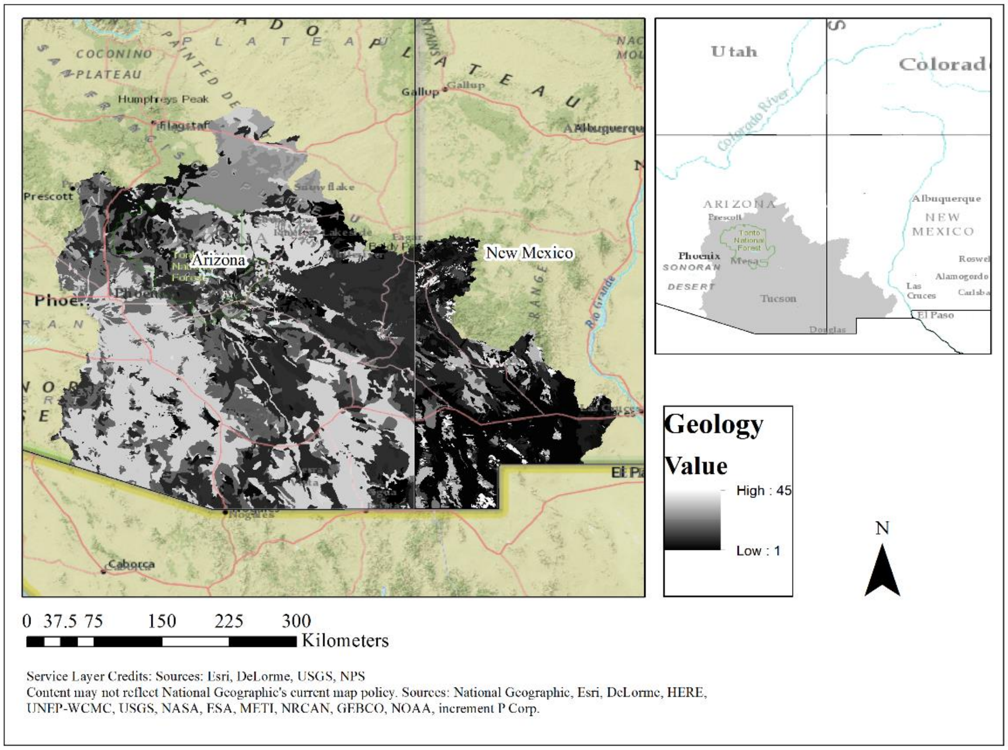

Figure U. Geology. See Table A for categories. (USGS 2005a, USGS 2005b)

Table A. Geology Categories (USGS 2005a, USGS 2005b)

Value	Rock Type
1	alkaline basalt
2	alluvium
3	andesite
4	basalt
5	carbonate
6	clastic
7	coarse-grained mixed clastic
8	conglomerate
9	dacite
10	diabase
11	eolian
13	felsic metavolcanic rock
14	felsic volcanic rock
16	gneiss
17	granite
18	granodiorite
19	gravel
20	greenstone
22	lake or marine deposit (non-glacial)
23	landslide
24	lava flow
25	limestone
27	medium-grained mixed clastic
29	mudstone
30	phyllite
32	plutonic rock (phaneritic)
33	pyroclastic
35	quartz monzonite
36	rhyolite
37	sand
38	sandstone
39	schist
40	sedimentary rock
41	shale
42	tuff
44	volcanic rock (aphanitic)
45	water

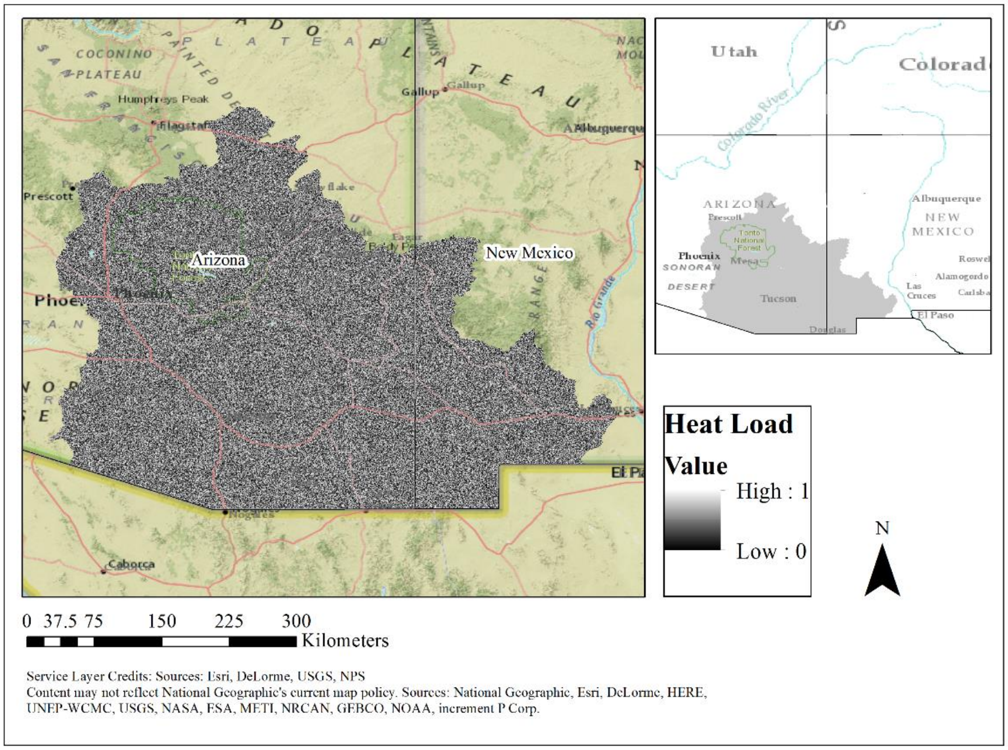

Figure V. Heat Load (= (1-cos(ɵ-45)) / 2), ɵ = aspect.

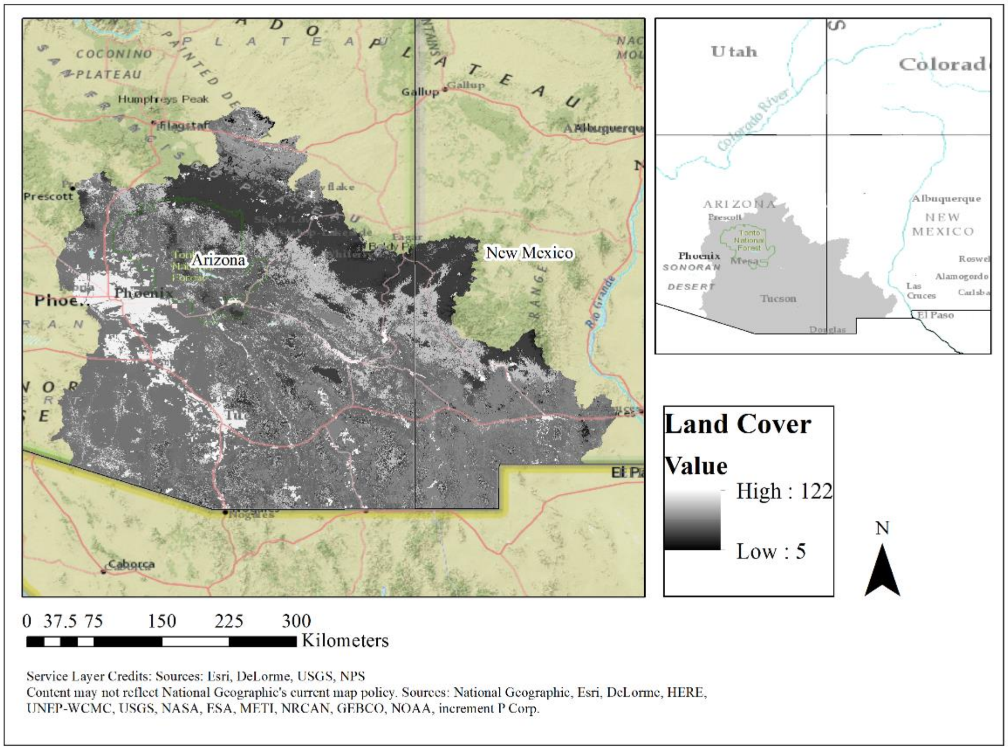

Figure W. Land cover. See Table B for categories. (USGS, 2004).

Table B. Land cover category descriptions. (USGS, 2004)

Value	Description
5	Rocky Mountain Cliff and Canyon
9	Colorado Plateau Mixed Bedrock Canyon and Tableland
10	Inter-Mountain Basins Shale Badland
12	Inter-Mountain Basins Volcanic Rock and Cinder Land
14	Inter-Mountain Basins Playa
15	North American Warm Desert Bedrock Cliff and Outcrop
17	North American Warm Desert Active and Stabilized Dune
18	North American Warm Desert Volcanic Rockland
19	North American Warm Desert Wash
20	North American Warm Desert Pavement
21	North American Warm Desert Playa
22	Rocky Mountain Aspen Forest and Woodland
24	Rocky Mountain Subalpine-Montane Limber-Bristlecone Pine Woodland
26	Rocky Mountain Subalpine Dry-Mesic Spruce-Fir Forest and Woodland
28	Rocky Mountain Subalpine Mesic Spruce-Fir Forest and Woodland
30	Rocky Mountain Montane Dry-Mesic Mixed Conifer Forest and Woodland
32	Rocky Mountain Montane Mesic Mixed Conifer Forest and Woodland
33	Madrean Pine-Oak Forest and Woodland
34	Rocky Mountain Ponderosa Pine Woodland
35	Southern Rocky Mountain Pinyon-Juniper Woodland
36	Colorado Plateau Pinyon-Juniper Woodland
41	Rocky Mountain Gambel Oak-Mixed Montane Shrubland
42	Rocky Mountain Lower Montane-Foothill Shrubland
45	Madrean Encinal
48	Inter-Mountain Basins Big Sagebrush Shrubland
50	Colorado Plateau Mixed Low Sagebrush Shrubland
51	Mogollon Chaparral
52	Apacherian-Chihuahuan Mesquite Upland Scrub
53	Colorado Plateau Blackbrush-Mormon-tea Shrubland
55	Chihuahuan Succulent Desert Scrub
56	Chihuahuan Creosotebush, Mixed Desert and Thorn Scrub
57	Sonoran Paloverde-Mixed Cacti Desert Scrub
58	Inter-Mountain Basins Mixed Salt Desert Scrub
59	Chihuahuan Stabilized Coppice Dune and Sand Flat Scrub
60	Sonora-Mojave Creosotebush-White Bursage Desert Scrub
61	Sonora-Mojave Mixed Salt Desert Scrub

64	Inter-Mountain Basins Juniper Savanna
65	Apacherian-Chihuahuan Piedmont Semi-Desert Grassland and Steppe
67	Inter-Mountain Basins Semi-Desert Shrub Steppe
68	Chihuahuan Gypsophilous Grassland and Steppe
71	Southern Rocky Mountain Montane-Subalpine Grassland
76	Inter-Mountain Basins Semi-Desert Grassland
79	Rocky Mountain Lower Montane Riparian Woodland and Shrubland
80	North American Warm Desert Lower Montane Riparian Woodland and Shrubland
82	Inter-Mountain Basins Greasewood Flat
83	North American Warm Desert Riparian Woodland and Shrubland
84	North American Warm Desert Riparian Mesquite Bosque
85	North American Arid West Emergent Marsh
86	Rocky Mountain Alpine-Montane Wet Meadow
91	Madrean Upper Montane Conifer-Oak Forest and Woodland
92	Madrean Pinyon-Juniper Woodland
93	Chihuahuan Sandy Plains Semi-Desert Grassland
95	Madrean Juniper Savanna
96	Chihuahuan Mixed Salt Desert Scrub
105	Sonoran Mid-Elevation Desert Scrub
108	Southern Colorado Plateau Sand Shrubland
110	Open Water
111	Developed, Open Space - Low Intensity
112	Developed, Medium - High Intensity
113	Barren Lands, Non-specific
114	Agriculture
116	Recently Burned
117	Recently Mined or Quarried
118	Invasive Southwest Riparian Woodland and Shrubland
122	Invasive Annual and Biennial Forbland

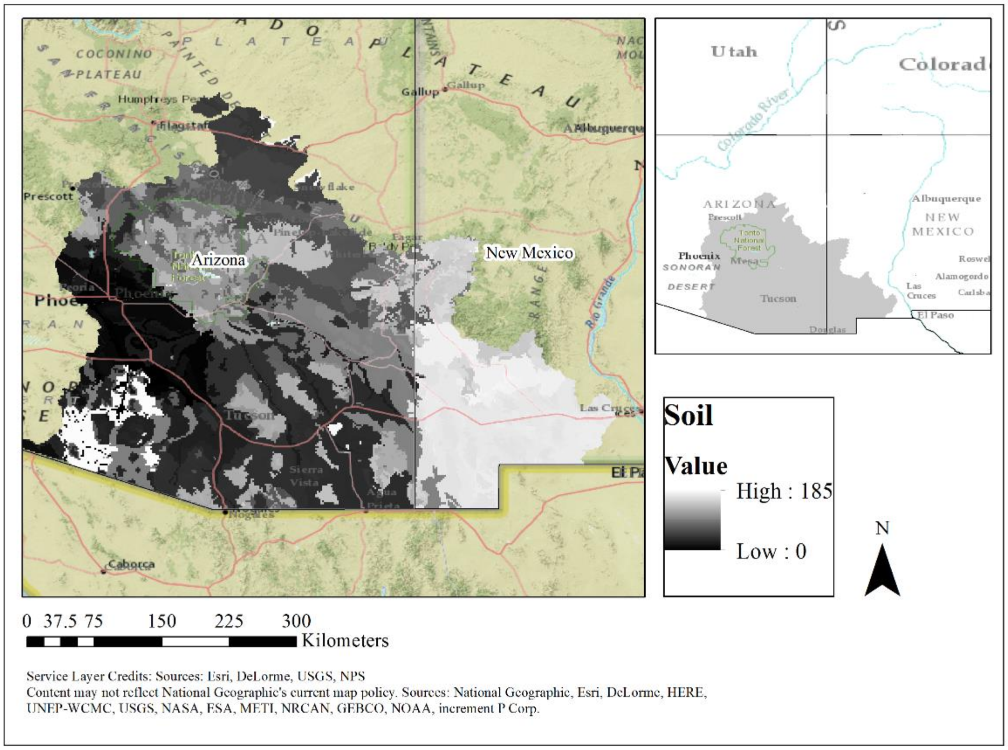

Service Layer Credits: Sources: Esri, DeLorme, USGS, NPS
Content may not reflect National Geographic's current map policy. Sources: National Geographic, Esri, DeLorme, HERE, UNEP-WCMC, USGS, NASA, ESA, METI, NRCAN, GEBCO, NOAA, increment P Corp.

Figure X. Soil. SSURGO. See Table C for definitions. (NRCS, 2016).

Table C. Soil series definitions (NRCS, 2016).

Value	Soil Series	Map Unit Key
0	Denure-Dateland (s276)	658354
1	Glenbar-Gadsden-Brios (s277)	658355
2	Sasco-Marana-Denure (s278)	658356
3	Yahana-Indio-Gadsden (s279)	658357
4	Pahaka-Mohall-Laveen-Denure (s280)	658358
5	Momoli-Denure-Carrizo (s281)	658359
6	Mohall-Denure-Coolidge (s283)	658361
7	Mohall-Contine (s284)	658362
8	Yahana-Shontik-Casa Grande (s285)	658363
9	Tremant-Pinamt-Ebon (s286)	658364
10	Suncity-Cipriano-Carefree (s287)	658365
11	Rillito-Gunsight-Denure-Chuckawalla (s288)	658366
12	Hyder-Coolidge-Cipriano-Cherioni (s289)	658367
13	Pinamt-Gunsight-Cavelt (s291)	658369
14	Pinamt-Momoli-Cipriano (s292)	658370
15	Rock outcrop-Quilotosa-Momoli (s293)	658371
16	Rock outcrop-Quilotosa-Hyder-Gachado (s294)	658372
17	Laveen-Kamato-Casa Grande (s296)	658374
18	Toltec-La Palma-Casa Grande (s297)	658375
19	Mohall-Dateland-Casa Grande (s298)	658376
20	Pahaka-Estrella-Antho (s299)	658377
21	Guest-Glendale-Gila (s302)	658380
22	Riveroad-Comoro-Arizo (s303)	658381
23	Sonoita-Hayhook-Continental (s307)	658385
24	Sahuarita-Mohave-Cave (s308)	658386
25	Stagecoach-Nahda-Delnorte-Agustin (s310)	658388
26	Pinaleno-Eba (s311)	658389
27	Pinaleno-Palos Verdes-Nickel (s313)	658391
28	Rock outcrop-Lehmans-Gran (s316)	658394
29	Rock outcrop-Lajitas-Delthorny-Anklam (s317)	658395
30	Santo Tomas-Pima-Comoro (s320)	658398
31	Hondale-Gothard-Bluepoint (s321)	658399
32	Sontag-Bonita (s322)	658400
33	Tubac-Forrest-Enzian-Diaspar (s323)	658401

34	White House-Hathaway-Bernardino (s325)	658403
35	Tombstone-Stronghold-Jerag (s326)	658404
36	White House-Hathaway-Caralampi-Bernardino (s328)	658406
37	Romero-Rock outcrop-Lampshire (s329)	658407
38	Rock outcrop-Mabray-Lemitar (s335)	658413
39	Tours saline-Sodic-Riverwash-Jocity saline-Sodic-Ives saline-Sodic-Burnswick (s337)	658415
40	Marcou-Jocity saline-Sodic-Burnswick (s338)	658416
41	Wepo-Polacca-Jocity-Jeddito (s339)	658417
42	Sheppard sodic-Sheppard-Joraibi-Jocity (s340)	658418
43	Purgatory-Epikom-Claysprings-Badland (s344)	658422
44	Winona-Tusayan-Boysag (s355)	658433
45	Rock outcrop-Needle-Epikom (s356)	658434
46	Wupatki-Wukoki-Tuweep (s360)	658438
47	Rock outcrop (s362)	658440
48	Sheppard-Grieta (s363)	658441
49	Ubank-Cerrillos-Barx (s366)	658444
50	Rock outcrop-Mellenthin-Leanto-Kech-Bisoodi (s367)	658445
51	Nuffel-Kech-Barx (s368)	658446
52	Rock outcrop-Deama (s369)	658447
53	Moano-Barkerville (s373)	658451
54	Typic Haplustalfs (s376)	658454
55	Thunderbird-Springerville-Rudd-Cabezon (s377)	658455
56	Springerville-Cabezon (s379)	658457
57	Poley-Pastura-Partri-Lynx-Abra (s381)	658459
58	Lynx-Lonti-Balon (s382)	658460
59	Telephone-Rock outcrop-Overgaard-Elledge (s385)	658463
60	Spudrock-Elledge-Docdee (s386)	658464
61	Gordo-Baldy (s387)	658465
62	Sponseller-Ess (s388)	658466
63	Thunderbird-Showlow (s389)	658467
64	Typic Haplustalfs-Rock outcrop-Aridic Haplustalfs (s390)	658468
65	Typic Haplustalfs-Lithic Haplustalfs (s391)	658469
66	Abreu (s395)	658473
67	Typic Eutroboralfs (s396)	658474
68	Typic Eutroboralfs (s397)	658475
69	Pinamt-Momoli-Hickiwan-Gunsight-Denure (s399)	658477

70	Retriever-Calciorthids (s400)	658478
71	Vertic Haplustalfs-Aridic Ustochrepts (s401)	658479
72	Rock outcrop-Lama-Fragua (s402)	658480
73	Winona-Spudrock-Rock outcrop (s403)	658481
74	Winona-Spudrock-Rock outcrop (s404)	658482
75	Quintana (s405)	658483
76	Typic Paleboralfs-Eutric Glossoboralfs (s406)	658484
77	Typic Cryoboralfs-Rock outcrop-Eutric Glossoboralfs (s407)	658485
78	Rock outcrop-Eutric Glossoboralfs (s408)	658486
79	Typic Paleboralfs-Typic Cryoboralfs-Rock outcrop (s411)	658489
80	Vertic Haplustalfs-Typic Haplustalfs (s412)	658490
81	Silkie-Espiritu (s416)	658494
82	Wineg-Quintana-Amos (s417)	658495
83	Typic Haplustalfs-Lithic Haplustalfs (s418)	658496
84	Mollic Eutroboralfs (s419)	658497
85	Rock outcrop-Mollic Cryoboralfs-Eutric Glossoboralfs (s420)	658498
86	Mirand-Derecho (s421)	658499
87	Vibo-Casto (s423)	658501
88	Typic Haplustalfs-Mollic Eutroboralfs (s424)	658502
89	Mirand-Maes (s425)	658503
90	Eutric Glossoboralfs (s426)	658504
91	Heflin-Casto (s427)	658505
92	Tombstone-Romero-Rock outcrop (s429)	658507
93	Tubac-Pajarito-Hayhook-Glendale-Bucklebar (s430)	658508
94	Tres Hermanos-Pinamt-Artesia (s431)	658509
95	Eicks-Eba-Cloverdale (s432)	658510
96	Limpia-Graham-Bonita-Atascosa (s433)	658511
97	Mabray-Chiricahua-Atascosa (s434)	658512
98	Rock outcrop-Mokiak-Faraway (s435)	658513
99	Rock outcrop-Luzena-Fallsam (s436)	658514
100	Tapco-Peloncillo-Artesia (s437)	658515
101	Wampoo-Signal-Bonita (s438)	658516
102	Selevin-Eloma-Alsco (s439)	658517
103	Abreu (s446)	658524
104	Altar (s447)	658525
105	Altar (s448)	658526

106	Rock outcrop-Garr (s449)	658527
107	Badland-Aridic Ustochrepts-Aridic Haplustolls (s453)	658531
108	Shoegame-McNeal-Badland (s454)	658532
109	Rock outcrop-Lithic Ustorthents family-Hogris (s455)	658533
110	Torriorthents-Cellar (s456)	658534
111	Spudrock-Rock outcrop-Cellar (s457)	658535
112	Yaqui-Werlog (s458)	658536
113	Werlog-Santo Tomas-Riverwash (s459)	658537
114	Torriorthents (s460)	658538
115	Typic Ustifluvents-Fluventic Ustochrepts (s462)	658540
116	Fluventic Ustochrepts-Aquic Ustifluvents (s463)	658541
117	Vessilla-Rock outcrop (s464)	658542
118	Teromote-Kopie (s465)	658543
119	Shoegame-Badland-Aridic Ustochrepts (s468)	658546
120	Typic Ustochrepts-Lithic Ustochrepts (s470)	658548
122	Typic Dystrochrepts-Dystric Cryochrepts (s473)	658551
123	Typic Dystrochrepts-Rock outcrop-Dystric Cryochrepts (s474)	658552
124	Sobega-Quintana-Kopie (s476)	658554
125	Dystric Cryochrepts (s477)	658555
126	Rock outcrop-Lithic Ustochrepts (s478)	658556
127	Typic Dystrochrepts-Rock outcrop-Lithic Ustochrepts (s479)	658557
128	Spudrock-Sobega-Rock outcrop (s481)	658559
129	Spudrock-Rombo-Rock outcrop (s482)	658560
130	Timhus-Quintana-Flugle (s483)	658561
131	Ess-Cundiyo (s485)	658563
132	Vertic Argiborolls (s487)	658565
133	Pachic Udic Argiborolls (s488)	658566
134	Rock outcrop-Lithic Haplustolls (s489)	658567
135	Nakai-Monue-Blackston (s490)	658568
136	Ustochreptic Calciorthids (s491)	658569
137	Faraway-Barkerville (s496)	658574
138	Tours-Showlow-Cibeque (s497)	658575
139	Rond-Jacks-Chevelon (s498)	658576
140	Tortugas-Roundtop-Rock outcrop (s499)	658577
141	Lemitar-Lampshire-Chiricahua (s500)	658578
142	Tuloso-Tinaja (s501)	658579

143	Riverwash-Prewitt-Pinetop-Lynx (s502)	658580
144	Typic Ustochrepts-Typic Haplustalfs (s5052)	665714
145	Vertic Haplustalfs-Typic Haplustalfs (s5061)	665723
146	Typic Haplustalfs-Aridic Haplustalfs (s5062)	665724
147	Typic Haplustalfs-Lithic Haplustalfs (s5063)	665725
148	Typic Eutroboralfs-Lithic Haplustalfs (s5065)	665727
149	Typic Haplustalfs-Rock outcrop-Eutric Glossoboralfs (s5068)	665730
150	Rock outcrop-Mollic Cryoboralfs-Eutric Glossoboralfs (s5075)	665737
151	Typic Haplustalfs-Mollic Eutroboralfs (s5076)	665738
152	Typic Ustifluvents-Fluventic Ustochrepts (s5082)	665744
153	Fluventic Ustochrepts-Aquic Ustifluvents (s5083)	665745
154	Typic Ustorthents-Typic Ustochrepts-Typic Udorthents-Rock outcrop (s5085)	665747
155	Typic Ustochrepts-Rock outcrop-Aridic Ustochrepts (s5087)	665749
156	Typic Ustochrepts-Fluventic Ustochrepts (s5088)	665750
157	Udic Ustochrepts-Typic Ustochrepts (s5094)	665756
158	Typic Dystrochrepts-Rock outcrop-Dystric Cryochrepts (s5100)	665762
159	Typic Ustochrepts-Rock outcrop-Lithic Ustochrepts-Aridic Ustochrepts-Aridic Haplustalfs (s5105)	665767
160	Typic Dystrochrepts-Rock outcrop-Lithic Ustochrepts (s5106)	665768
161	Fluventic Haploborolls-Aquic Ustifluvents (s5108)	665770
162	Typic Argiborolls (s5116)	665778
163	Seis-Rock outcrop-Orthids-Carlito (s5223)	665885
164	Tome-Mimbres (s5271)	665933
165	Rock outcrop-Lehmans-Chiricahua-Chamberino (s5315)	665977
166	Rock outcrop-Lehmans (s5316)	665978
167	Rock outcrop-Ledru-Graham (s5317)	665979
168	Nickel (s5319)	665981
169	Stellar-Mohave-Mimbres-Berino (s5320)	665982
170	Hondale (s5321)	665983
171	Wink-Pintura-Bluepoint (s5322)	665984
172	Upton-Simona (s5323)	665985
173	Rock outcrop-Lava flows-Akela-Aftaden (s5324)	665986
174	Rock outcrop-Muzzler-Luzena (s5325)	665987

175	Lonti-Jonale-Deama (s5326)	665988
176	White House-Ruidoso-Paymaster-Manzano-Judd (s5327)	665989
177	Scholle-Millett-Ildefonso-Goldust-Cascajo (s5328)	665990
178	Plack-Guy (s5329)	665991
180	Loarc-Guy-Dioxice-Datil (s5396)	666058
181	Water (s8369)	657964
182	Leanto-Bisoodi-Arntz (s9582)	804813
183	Torriorthents-Marcou-Claysprings-Burnswick-Badland (s9583)	804816
184	Vecont-Trix-Mohall-Denure-Dateland-Casa Grande (s9585)	806441
185	Selevin-Kimrose-Keysto-Caralampi (s9586)	806442